

This document was prepared in conjunction with work accomplished under Contract No. DE-AC09-76SR00001 with the U.S. Department of Energy.

### **DISCLAIMER**

This report was prepared as an account of work sponsored by an agency of the United States Government. Neither the United States Government nor any agency thereof, nor any of their employees, makes any warranty, express or implied, or assumes any legal liability or responsibility for the accuracy, completeness, or usefulness of any information, apparatus, product or process disclosed, or represents that its use would not infringe privately owned rights. Reference herein to any specific commercial product, process or service by trade name, trademark, manufacturer, or otherwise does not necessarily constitute or imply its endorsement, recommendation, or favoring by the United States Government or any agency thereof. The views and opinions of authors expressed herein do not necessarily state or reflect those of the United States Government or any agency thereof.

This report has been reproduced directly from the best available copy.

Available for sale to the public, in paper, from: U.S. Department of Commerce, National Technical Information Service, 5285 Port Royal Road, Springfield, VA 22161, phone: (800) 553-6847, fax: (703) 605-6900, email: [orders@ntis.fedworld.gov](mailto:orders@ntis.fedworld.gov) online ordering: <http://www.ntis.gov/ordering.htm>

Available electronically at <http://www.doe.gov/bridge>

Available for a processing fee to U.S. Department of Energy and its contractors, in paper, from: U.S. Department of Energy, Office of Scientific and Technical Information, P.O. Box 62, Oak Ridge, TN 37831-0062, phone: (865) 576-8401, fax: (865) 576-5728, email: [reports@adonis.osti.gov](mailto:reports@adonis.osti.gov)

TECHNICAL DIVISION  
SAVANNAH RIVER PLANT

DPST-81-732

DISTRIBUTION: See cover sheet

*Acc. No. 139830*

TO: D. A. WARD

October 26, 1981

FROM: J. L. STEIMKE

*J. L. Steimke*

POWER LIMITS FOR REACTOR ASSEMBLIES  
IN ABSENCE OF FORCED COOLING

TIS FILE  
RECORD COPY

SUMMARY

Forced cooling power limits for seven assembly types were calculated. The forced cooling limit is the amount of heat that can be safely removed from an assembly in a reactor in the absence of forced cooling. Heat removal is presumed to be by natural convection only. Assembly forced cooling limits were calculated to satisfy the present procedural criterion that the maximum coolant temperature in the assembly never exceed 100°C. Alternate limits were calculated for a proposed temperature limit of 106°C, the local saturation temperature of D<sub>2</sub>O at the top of the fuel or target columns in the assemblies. After approval of this memorandum, Technical Specification 105-2.7 will be changed to increase the maximum allowable D<sub>2</sub>O temperature to the local saturation temperature of D<sub>2</sub>O. Table 4.05-I of the Technical Standards will be changed to contain the new forced cooling limits. The heat transfer process in each reactor assembly type was analyzed and described by a number of equations which were derived from first principles or from established heat transfer correlations. The equations contained no adjustable constants. The set of equations was solved simultaneously. The solution gave temperatures at various points in the assembly and coolant velocities resulting from natural convection, all as functions of assembly power. Power limits were calculated subject to the maximum temperature limits.

The correctness of the analytical method was verified with experimental data for two assembly types. For the experiments a full scale mockup was made of the Mark 31A assembly. It was easily converted to a mockup of the Mark 31B assembly. The mockup was instrumented and placed in

A-Tank in the Heat Transfer Lab (HTL). After filling the tank with light water, the target columns in the mockup were electrically heated and temperature and convective velocity data were taken for both assembly types and for a series of assembly powers and tank water temperatures. The temperatures and velocities calculated by the analytical method agreed well with the experimental data. This good agreement validated the analytical method. It gave strong confidence that the method could be used for any SRP assembly type. Then the same method was used with heavy water properties for the Mark 31A, 31B, 16, 16B, 53A, and 22 assemblies to calculate forced cooling limits. The limits listed in Table I are conservative because they are based on no coolant boiling. A limited amount of boiling would be harmless and would enhance heat transfer in two ways. First, the presence of vapor bubbles in the inner annuli of an assembly would increase the density difference between the coolant in the inner annuli and the outer annulus. This would drive the circulation inside the assembly faster. Second, the mixing caused by bubbles growing and quenching would stir the coolant in the annuli which would increase heat transfer coefficients.

#### INTRODUCTION

Several hours after nuclear shutdown of the reactors the process water circulation is reduced to normal charge-discharge (CD) flow. Normal CD flow is the flow from three or four process water pumps with DC drive and throttled rotovalves. During a complete reactor core discharge or during a partial core discharge accompanied by the failure of a process water pump it is possible for some assemblies to be starved for flow. In these cases, the only mechanism for heat removal is natural convection inside and outside the affected assemblies. The power that can be dissipated from an assembly by natural convection without overheating the assembly is the forced cooling limit. Reactor Department procedures prohibit group discharge of assemblies until the power of the most restrictive assembly has decayed to the forced cooling limit. Therefore the forced cooling limit determines the length of the waiting time before group discharge can begin. RRMT requested a calculation of forced cooling limits for the primary assembly types.

This document reports the results of an experimental and analytical study done to provide the forced cooling limits for all presently used reactor assemblies.

DISCUSSIONDesign of test assemblies

The Mark 31A assembly consists of two concentric target columns, an inner housing and a bottom fitting insert inside a Universal Sleeve Housing (USH) as shown in Figure 1. The test assembly which simulated the Mark 31A used a standard USH and bottom fitting insert. The inner housing was machined from a solid rod of polyester glass. Replica target columns were made from type 304L stainless steel. Stainless steel was chosen because it was readily available, had a convenient electrical resistivity and had a thermal conductivity similar to that of uranium. The target columns were machined as short segments. The segments were welded together to provide electrical continuity necessary for resistance heating. Grooves were machined in the target columns and the inner housing. Strips of polyester glass were fastened in the grooves to form ribs. The ribs isolated the USH and target columns electrically and formed coolant channels.

Electrical power for resistance heating was supplied by two power rectifiers in the HTL. Bus connectors inside A-tank were connected to copper studs in the tops and bottoms of the target columns with braided copper cables. Brass end pieces were silver-soldered to the top and bottom of each column to give a better connection with the copper studs. The copper studs passed through holes drilled in the USH. The USH holes were drilled oversize to prevent current from shorting through the USH. To prevent water leakage through the gaps created by the oversize holes the gaps were plugged with Teflon (Du Pont trademark) gaskets. The target columns were electrically isolated at the bottom by replacing the standard metal target spacer which supports them with one made from Teflon. The target columns were electrically connected in parallel. A simple parallel circuit would have generated proportionately too much heat in the inner housing. Therefore, the heat production in the inner target column was reduced by adding another resistance in series with the inner target column. The extra resistance was a one foot length of one inch Sch. 40 stainless steel pipe. That adjustment gave the inner column the correct percentage of the total heat production, 26.9%.

The Mark 31A test assembly was easily converted to Mark 31B configuration. First, electrical power was disconnected from the inner target column. It then simulated the Mark 31B inner housing. Second, the annulus just inside the inner target column was blocked to prevent flow through it.

### Instrumentation of test assembly

The test assembly was instrumented with electrical conductivity probes for fluid velocity measurements and thermocouples. The test assembly held eight thermocouples, one each in the top and bottom of the three annuli, and one each in the top of the two target columns. In addition, there were three thermocouples in the water surrounding the assembly, at the top, bottom, and mid-height. The test assembly also held six electrical conductivity probes; one each at the bottom of the three annuli and one each at the top of the three annuli. Each conductivity probe consisted of two wires whose bare tips were positioned one-quarter inch apart. The conductivity probes were used to measure the length of time required for a salt tracer to be carried from one end of the assembly to the other. The salt solution consisted of 40 g of LiCl, 140 ml of ethanol and 900 ml of H<sub>2</sub>O. The ethanol was added to give the salt solution neutral buoyancy in water. The solution was heated to approximately match the water temperature inside the assembly. Several milliliters of solution were injected in the top or bottom of an annulus and carried past the two conductivity probes. An electrical circuit, shown in Figure 2, was designed to monitor the conductivity across the probes. The signal from the circuit was recorded on a strip chart recorder as shown in Figure 3.

### Instrument Calibrations

The following instruments were calibrated; the thermocouples and the digital thermocouple reading device, the strip chart recorder, the rectifier voltmeter and the rectifier current meters. Also the salt injection method for measuring fluid velocities was calibrated. Discussion and results of the calibrations are listed in Appendix A.

## ANALYSIS OF NATURAL CONVECTION HEAT TRANSFER IN MARK 31A ASSEMBLY

The Mark 31A assembly was modeled as four concentric tubes. During certain circumstances it is possible to have no flow in or out of the USH. Therefore for the purposes of modeling the USH was assumed to be sealed at both ends. The model of the assembly is shown in Figure 4. The surfaces are labeled one through five and the annuli are labeled A, B, and C.

The solution to the problem satisfied conservation of mass and energy, hydraulics relations and heat transfer relations. The first part of heat transfer problem was the cooling of

the outside of the USH by natural convection in the moderator. The heat transfer relation for natural convection from the vertical surface was<sup>1</sup>

$$\text{Nu} = .13(\text{Gr}_L \text{Pr})^{1/3}$$

valid when  $10^9 < \text{Gr}_L \text{Pr} < 10^{12}$   
 where  $\text{Nu} = hL/k$

$$\text{Gr}_L = \frac{L^3 \rho^2 g \beta (\bar{T}_s - T_w)}{\mu^2}$$

$$\text{Pr} = c_p \mu / k$$

$h$  = heat transfer coefficient, PCU/ft<sup>2</sup> hr°C

$L$  = length of cylinder, ft.

$\rho$  = density, lb/ft<sup>3</sup>

$k$  = thermal conductivity, PCU/ft hr°C

$g$  = acceleration of gravity, ft/hr<sup>2</sup>

$\beta$  = coefficient of thermal expansion 1/°C

$\bar{T}_s$  = average temperature at surface, °C

$T_w$  = fluid temperature away from surface, °C

$c_p$  = heat capacity of fluid, PCU/lb°C

$\mu$  = viscosity, lb./ft. hr.

The properties  $k$ ,  $\mu$  and  $\beta$  were evaluated at the film temperature  $T_f$ , where

$$T_f = (\bar{T}_s + T_w)/2.$$

The rate of heat loss from the portions of the USH covering the heated fuel elements was

$$Q_u = D k \pi .13 (\text{Gr Pr})^{1/3} (\bar{T}_s - T_w) \quad [1]$$

where  $D$  was the diameter. Equation 1 was used to solve for the unknown average USH temperature,  $\bar{T}_s$ . Once evaluated,  $\bar{T}_s$  was treated as a constant in the simultaneous solution

of the governing set of equations as derived in the remainder of the report.

Inside the USH, a convective flow pattern formed. The fluid in the annulus between the USH and the outer target columns was the coolest and most dense fluid in the assembly because it was the only fluid in thermal contact with the cool tank water. Therefore, the flow was downward in the outermost annulus. This was balanced by upflows in the inner and middle annuli. Heat from the target tubes was transferred to the fluid in the upflow annuli. The liquid in the upflow annuli mixed at the top of the assembly and flowed down the outermost annulus where it cooled. At the bottom of the assembly the liquid turned upward and the cycle repeated. The total mass flow rate in the upflow channels was equal to the mass flow rate in the downflow channel. The conservation of mass relation is:

$$U_A A_A + U_B A_B = U_C A_C \quad [2]$$

where  $A_A$ ,  $A_B$  and  $A_C$  are cross-sectional areas of the three annuli and  $U_A$ ,  $U_B$  and  $U_C$  are velocities.

The assembly hydraulics involved a balance of driving forces caused by density differences and viscous resisting forces. There are two coupled flow loops in the assembly, annuli A and C taken together and annuli B and C taken together. The flows in the annuli were laminar so that the pressure drop in one annulus is given by (2):

$$\begin{aligned} \Delta P_A &= F_A U_A \\ \Delta P_B &= F_B U_B \\ \Delta P_C &= F_C U_C \end{aligned} \quad [3]$$

where

$$F = \frac{8\mu L}{g r_o^2 \left( \frac{1-k^4}{1-k^2} - \frac{1-k^2}{\ln \frac{1}{k}} \right)}$$

where  $r_o$  = outer radius of annulus in question

$r_i$  = inner radius

$k = r_i/r_o$

The total pressure drops for flow loops AC and BC are:

$$\begin{aligned}\Delta P_{AC} &= F_A U_A + F_C U_C \\ \Delta P_{BC} &= F_B U_B + F_C U_C\end{aligned}\quad [4]$$

The annular radii are listed in Table II. There were additional pressure losses from the sudden contraction and sudden expansion at the entrance and exit of the annulus. These losses are approximated by

$$\Delta P_{cont} = \Delta P_{exp} \cong \frac{\rho U^2}{2g}$$

For any flow loop the driving pressure is equal to the total laminar pressure drop plus two sudden contraction losses plus two sudden expansion losses. However, the expansion and contraction losses were negligibly small for the range of velocities encountered.

The driving force for flow is the difference in weight of two columns of fluid. The static head differences between annuli A and C and annuli B and C at the assembly bottom are :

$$\begin{aligned}\Delta P_{AC} &= \int_0^L \rho_c(z) dz - \int_0^L \rho_A(z) dz \\ \Delta P_{BC} &= \int_0^L \rho_c(z) dz - \int_0^L \rho_B(z) dz\end{aligned}\quad [5]$$

Density was expanded in the form

$$\rho(T) = \rho_0 - (T - T_0) \rho_0 \beta$$

where  $\rho_0$  is the density at reference temperature  $T_0$ . Substituting gives :

$$\begin{aligned}\Delta P_{AC} &= \rho_0 \beta \left[ \int_0^L T_A(z) dz - \int_0^L T_C(z) dz \right] \\ \Delta P_{BC} &= \rho_0 \beta \left[ \int_0^L T_B(z) dz - \int_0^L T_C(z) dz \right]\end{aligned}\quad [6]$$

Two approximations were made at this point to make the solution more tractable. The first approximation was that temperature increased in a linear way with height in the two inner annuli, A and B. This was justified because heat production along those annuli was uniform for the experimental situation being modeled. Actual reactor assemblies have non-uniform heat production. A correction for this fact was made later. The results of the first approximation are :

$$\int_0^L T_A(z) dz = \frac{L}{2} [T_A(L) + T_A(0)] \quad [7]$$

$$\int_0^L T_B(z) dz = \frac{L}{2} [T_B(L) + T_B(0)] \quad [8]$$

The equations were simplified somewhat by noting that fluid leaving the bottom of annulus C immediately turned upward and entered annuli A and B. Therefore,

$$T_A(0) = T_B(0) = T_C(0)$$

The common bottom temperature is labeled  $T(0)$ .

The second approximation was that net local heat losses from the outer annulus were proportional to the temperature difference between the fluid in the outer annulus and the fluid surrounding the USH. There were actually two heat transfer processes in series. The first was from annulus C to the USH and the second was from the USH to the tank water. Because both heat transfer relationships were approximately linear functions of temperature drop the combined relationship was also linear. The net local heat loss from annulus C is approximated

$$(q_5 r_5 - q_4 r_4) 2\pi \Delta z = C_1 (T_c(z) - T_w) \Delta z \quad [9]$$

where  $C_1$  is a linearizing factor. The heat losses caused the fluid temperature to decrease as the fluid flowed down annulus C.

$$C_p \rho U_c \Delta z \frac{dT_c(z)}{dz} = (q_5 r_5 - q_4 r_4) 2\pi \Delta z \quad [10]$$

Equating equations 9 and 10 gives :

$$\frac{dT_c(z)}{dz} = C_3 (T_c(z) - T_w) \quad [11]$$

where  $C_3 = \frac{C_1}{C_p \rho U_c}$ . The solution of equation 11 is

$$T_c(z) = T_w + C_4 \exp(C_3 z)$$

or after substituting boundary conditions for  $T_c$

$$T_c(z) = T_w + (T(0) - T_w) \exp\left[\frac{z}{L} \ln\left(\frac{T_c(L) - T_w}{T(0) - T_w}\right)\right]$$

Integrating equation 12 gives:

$$\int_0^L T_c(z) dz = L T_w + \frac{L(T_c(L) - T(0))}{\ln \frac{T_c(L) - T_w}{T(0) - T_w}} \quad [13]$$

Constants  $C_3$  and  $C_4$  drop out of the solution.

The driving force for flow in both flow loops was found by substituting equations 7, 8, and 13 in equations 5 and 6. Equating the frictional resisting pressure drop to the driving force gave the desired equations.

$$F_A U_A + F_c U_c = \rho_o \beta L \left[ \frac{1}{2} (T_A(L) + T(0)) - T_w - \frac{T_c(L) - T(0)}{\ln \frac{T_c(L) - T_w}{T(0) - T_w}} \right] \quad [14]$$

$$F_B U_B + F_c U_c = \rho_o \beta L \left[ \frac{1}{2} (T_B(L) - T(0)) - T_w - \frac{T_c(L) - T(0)}{\ln \frac{T_c(L) - T_w}{T(0) - T_w}} \right] \quad [15]$$

Several equations were used to satisfy conservation of energy. The target columns lost heat from both the inner and outer surfaces. At steady state the sum of the two rates of surface heat loss is equal to the rate of heat production from that tube.

$$Q_1 + Q_2 = Q_I \quad [16]$$

$$Q_3 + Q_4 = Q_O \quad [17]$$

I and O refer to inner and outer target columns. The fluid in each channel increased in temperature in proportion to the amount of heat entering the channel.

$$Q_1 = U_A A_A \rho C_p (T_A(L) - T(0)) \quad [18]$$

$$Q_2 + Q_3 = U_B A_B \rho C_p (T_B(L) - T(0)) \quad [19]$$

$$Q_5 - Q_4 = U_C A_C \rho C_p (T_C(L) - T(0)) \quad [20]$$

where  $A_A$ ,  $A_B$ , and  $A_C$  are cross-sectional areas of annuli.

Eleven equations are necessary to describe the heat transfer relationships in the assembly. The first heat transfer mechanism is simple conduction in the target columns. The differential equation is  $-\phi r dr = k d\left(r \frac{dT}{dr}\right)$

with the boundary conditions that

$$\phi \pi (r_o - r_i) \Delta z = 2\pi (r_i q_i + r_o q_o) \Delta z$$

where  $\phi$  is the volumetric rate of heat generation. The solution is

$$T_i - T_o = \frac{r_i q_i}{k} \left[ .5 - \frac{r_o^2}{r_o^2 - r_i^2} \ln \frac{r_o}{r_i} \right] + \frac{r_o q_o}{k} \left[ .5 - \frac{r_i^2}{r_o^2 - r_i^2} \ln \frac{r_o}{r_i} \right] \quad [21]$$

where i and o refer to inner and outer surfaces and  $q_i$  and  $q_o$  are heat fluxes out surfaces, respectively. Heat flux  $q$  and surface heat loss  $Q$  are related by

$$Q = 2\pi r \int_0^L q(z) dz \quad [22]$$

The approximation was made that surface temperature varied linearly with height. Integrating equation 22 over height, substituting equation 21 and simplifying gave an equation for the inner target column.

$$.5 [T_1(L) + T_1(0) - T_2(L) - T_2(0)] = \frac{1}{2\pi L k} \left\{ Q_1 \left[ .5 - \frac{r_2^2}{r_2^2 - r_1^2} \ln \frac{r_2}{r_1} \right] + Q_2 \left[ .5 - \frac{r_1^2}{r_2^2 - r_1^2} \ln \frac{r_2}{r_1} \right] \right\} \quad [23]$$

For the outer target column the equation is

$$.5 [T_3(L) + T_3(0) - T_4(L) - T_4(0)] = \frac{1}{2\pi L k} \left\{ Q_3 \left[ .5 - \frac{r_4^2}{r_4^2 - r_3^2} \ln \frac{r_4}{r_3} \right] + Q_4 \left[ .5 - \frac{r_3^2}{r_4^2 - r_3^2} \ln \frac{r_4}{r_3} \right] \right\} \quad [24]$$

Calculations indicated that heat losses from the portion of the USH inside the shield and plenum were negligibly small and were therefore neglected. The heat loss by natural convection from the portion of the USH with length  $L'$  between the top of the heated target column and the bottom of the shield is:

$$Q_{TOP} = Q_T - Q_S = \pi D k .13 (Gr_{L'}, Pr)^{1/3} (T_S - T_w) \quad [25]$$

$L'$  is .33 ft for the Mark 31A and 31B assemblies. Some of the experimental data was taken at a second value of  $L'$ , one foot.

Heat transfer coefficients to annuli A and B were calculated with a correlation for laminar flow in tubes where buoyancy effects were important.<sup>3</sup> No correlation specifically for an annular geometry could be found. Equivalent diameters were substituted for tube diameters in the correlation. The correlation is

$$Nu = 2.246 + 1.45 (.785 Re' Pr D_e/L)^{1/3} \quad [26]$$

$$\text{where } Re' = \frac{U D_e \rho}{\mu} + .02 \frac{Gr^{.8}}{Pr^{.2}} \left( \frac{L}{D_e} \right)^{.2}$$

$$D_e = 2(r_o - r_i)$$

$$Gr = \frac{D_e^3 \rho^2 g \beta \Delta T}{\mu^2}$$

The local heat fluxes for surfaces 1 and 2 are

$$q_1(z) = h_1 [T_1(z) - T_A(z)] \quad [27]$$

$$q_2(z) = h_2 [T_2(z) - T_B(z)] \quad [28]$$

The approximation was again made that surface temperature varied linearly with height. Integrating equation 27 over height, substituting equation 21 and simplifying gives

$$Q_1 = \pi r_1 L h_1 [T_1(L) + T_1(0) - T_A(L) - T(0)] \quad [29]$$

Similarly

$$Q_2 = \pi r_2 L h_2 [T_2(L) + T_2(0) - T_B(L) - T(0)] \quad [30]$$

$$Q_3 = \pi r_3 L h_3 [T_3(L) + T_3(0) - T_B(L) - T(0)] \quad [31]$$

Annulus C was different from the other two because it had a heat source at the inner wall and a heat sink at the outer wall. There was experimental evidence that the flow pattern in annulus C was more complicated than the nearly parabolic flow profile expected in annuli A and B. When salt tracer

was injected in the top of the annulus it dispersed twice as fast as was expected for a simple laminar flow down the annulus. The most likely explanation was that there was a closed cell convection loop superimposed on the bulk flow down the annulus. The flow direction is down next to the inside of the relatively cool USH and up next to the hot outer target column. Numerous experiments reported in the technical literature have shown that when a heat flux is impressed across an annulus blocked at both ends a convection loop forms, up on the hot side and down on the cool side. The case of heat transfer between parallel plates is nearly identical and has been studied thoroughly. A heat transfer correlation<sup>4</sup> for natural convection of water between parallel plates was used because the annular gap in the assemblies was small.

$$Nu = .122 (Gr Pr)^{.29}$$

where  $Gr = \frac{x^3 \rho^2 g \beta (T_4 - T_5)}{\mu^2}$

x = Plate or annulus spacing

The average heat flow across annulus C was calculated from

$$(Q_4 + Q_5)/2 = \frac{2\pi r_c L k}{x} .122 (Gr Pr)^{.29} (T_4(L) - T_5(L)) \quad [32]$$

where  $r_c$  was the radius of the middle of the annulus.

The total heat loss for the top differential length of the inner target column is equal to the heat production.

$$\frac{Q_I \Delta Z}{L} = h_1 \Delta Z 2\pi r_1 \{T_1(L) - T_A(L)\} + h_2 \Delta Z 2\pi r_2 \{T_2(L) - T_B(L)\} \quad [33]$$

Similarly the equation for the outer target column is

$$\frac{Q_O \Delta Z}{L} = h_3 \Delta Z 2\pi r_3 \{T_3(L) - T_B(L)\} + h_4 \Delta Z 2\pi r_4 \{T_4(L) - T_C(L)\} \quad [34]$$

Another pair of independent equations were derived to relate heat conduction at the tops of the target columns with heat convection at their surfaces. Equations 27 and 28 were substituted in 21 where the inner and outer surfaces are 1 and 2 respectively.

$$T_1(L) - T_2(L) = \frac{r_1 h_1}{k} [T_1(L) - T_A(L)] \left( .5 - \frac{r_2^2}{r_2^2 - r_1^2} \ln \frac{r_2}{r_1} \right) + \frac{r_2 h_2}{k} [T_2(L) - T_B(L)] \left( .5 - \frac{r_1^2}{r_2^2 - r_1^2} \ln \frac{r_2}{r_1} \right) \quad (35)$$

Similarly

$$T_3(L) - T_4(L) = \frac{r_3 h_3}{k} [T_3(L) - T_B(L)] \left( .5 - \frac{r_4^2}{r_4^2 - r_3^2} \ln \frac{r_4}{r_3} \right) + \frac{r_4 h_4}{k} [T_4(L) - T_C(L)] \left( .5 - \frac{r_3^2}{r_4^2 - r_3^2} \ln \frac{r_4}{r_3} \right) \quad [36]$$

The set of equations was completed by two which described temperature relationships. The bulk temperature of the coolant at the top of annulus C is approximately equal to the average of the enclosing metal temperatures.

$$T_C(L) = [T_4(L) + T_5(L)]/2 \quad [37]$$

The USH temperature at mid height is equal to the average temperature in annulus C minus half the difference between  $T_4$  and  $T_5$ .

$$\bar{T}_5 = [T_C(L) + T(0)]/2 - [T_4(L) - T_5(L)]/2. \quad [38]$$

Some of the equations derived above contained non-linear terms and were linearized to allow solution by matrix inversion. Equations 18, 19, 20 contained terms with velocity multiplied by a temperature difference. They were linearized with a Taylor series expansion. The equations were rewritten

$$\frac{Q_1}{A_A \rho C_P} = U_{A0} \{T_A(L) - T_o(0)\} + U_A \{T_{A0}(L) - T_o(0)\} - U_{A0} \{T_{A0}(L) - T_o(0)\} \quad [39]$$

$$\frac{Q_2 + Q_3}{A_B \rho C_P} = U_{B0} \{T_B(L) - T_o(0)\} + U_B \{T_{B0}(L) - T_o(0)\} - U_{B0} \{T_{B0}(L) - T_o(0)\} \quad [40]$$

$$\frac{Q_5 - Q_4}{A_C \rho C_P} = U_{C0} \{T_C(L) - T_o(0)\} + U_C \{T_{C0}(0) - T_o(0)\} - U_{C0} \{T_{C0}(L) - T_o(0)\} \quad [41]$$

where the subscript o denoted an initial guess which was updated in subsequent iterations. Equations 14 and 15 contained terms with natural logarithms. The temperatures in the logarithm terms were originally estimated, then updated in subsequent iterations. Many equations contained heat transfer coefficients which were functions of physical properties and temperature differences. They were handled in the same way.

The analysis produced 21 independent, quasi-linear equations in 21 unknowns, summarized as follows.

Equations

Conservation of mass	2
Conservation of momentum (buoyancy)	14, 15
Conservation of energy	16, 17
Heat transfer relations	23, 24, 25, 29, 30, 31, 32, 33, 34, 35, 36, 39, 40, 41
Temperature relationships	37, 38

Unknowns

Velocities	$U_A, U_B, U_C$
Heat flows	$Q_1, Q_2, Q_3, Q_4, Q_5$
Temperatures	$T_1(L), T_2(L), T_3(L), T_4(L),$ $T_5(L), T_1(0), T_2(0), T_3(0),$ $T_4(0), T_A(L), T_B(L), T_C(L),$ $T(0)$

Solution of the equation set was as follows. First, equation 1 was solved for  $\bar{T}_5$ . Second, estimates were made of the variables involved in the non-linear terms. The resulting set of linear equations was solved by matrix inversion. The solutions for the variables were then substituted into the non-linear terms again and the cycle repeated. Convergence to the true solution required about ten iterations. A computer program MK31AX was written to solve the equations and is given in Appendix B.

It was convenient to write a different program for each type of assembly considered. To solve the Mark 31B problem the set of equations for the Mark 31A assembly was altered by

removing all references to the inner target column and annulus A. Eight variables disappeared;  $T_1(L)$ ,  $T_2(L)$ ,  $T_1(0)$ ,  $T_2(0)$ ,  $T_A(L)$ ,  $U_A$ ,  $Q_1$ , and  $Q_2$ . Thirteen equations remained and were solved.

#### Comparison of Experimental Data and Analysis

Heat transfer processes in the Mark 31A and 31B assemblies were analyzed with the process outlined in this memorandum. Light water properties were used in the analyses. Temperatures and velocities were calculated in the assemblies. These were compared with experimentally measured temperatures and velocities. Experiments and analytical calculations were done for two different values of  $L'$ , the distance from the top of the heated section of the assemblies to the shield. Originally it was thought that  $L'$  was equal to one foot. Later the distance of one foot was corrected to four inches. That change made a small difference in both experimentally observed and calculated assembly temperatures. Data are presented for values of  $L'$  of both one foot and four inches. The data for one foot were retained and presented because they provide additional verification for the analytical model.

To verify the accuracy of the computer model the results of the model were compared with experimental data for both moderator levels and for tank water temperatures of 30°C and 50°C. For the Mark 31A assembly, temperatures measured at six locations and velocities measured at three locations were compared with the corresponding calculated temperatures and velocities at the same locations. The agreement ranged from good to excellent. The temperature data for two locations and velocity data at one location will be presented.

Experimental data for both Mark 31A and 31B assemblies and results of the computer model are shown in Figures 5 through 10. Figures 5 and 6 show the difference between the maximum water temperature (at surface 1) referenced to tank water temperature. Agreement between data and model is excellent for most of the eight data sets. For the Mark 31B with a moderator level of four inches and  $T_w = 50^\circ$  the model overpredicted temperature, which is a conservatism. Figures 7 and 8 show the temperature at the top of the outer annulus referenced to tank water temperature. Agreement between the experimental data and model results is good. Figures 9 and 10 show the convective velocity in annulus B. Agreement is good at low powers. At higher powers the model overestimated velocity. A possible source of the discrepancy was the

assumption of simple laminar flow in equations 3 for resistance to flow. At higher powers buoyancy effects were increasingly important and made the flow pattern more complicated. The actual resistance to flow was probably higher than the resistance used in the model.

SOLUTIONS TO HEAT TRANSFER PROBLEMS  
IN OTHER ASSEMBLIES

The analytical method developed for the Mark 31A and 31B assemblies was used for the Mark 16, 16B, 15, and 53A assemblies. A similar but different method was used for the Mark 22 assembly. In each case heavy water properties and the appropriate value of  $L'$  were used.

Mark 16 and 16B

The two assemblies were structurally identical with small differences in power splits between the fuel tubes. They contained one more tube than the Mark 31A. This would have meant eight more variables and equations than the Mark 31A. However, the fact that the fuel tubes were mostly aluminum simplified the problem. The high thermal conductivity meant that the temperature difference across a tube was a few tenths of a degree and thus negligible. Therefore, variables  $T_2(L)$ ,  $T_2(0)$ ,  $T_4(L)$ ,  $T_4(0)$ ,  $T_6(L)$ , and  $T_6(0)$ , were deleted leaving 23 equations.

Mark 15

The Mark 15 was geometrically similar to the Mark 31A and required 21 equations.

Mark 53A

The Mark 53A was geometrically similar to the Mark 31B. This would have meant thirteen equations. However the high thermal conductivity of the tubes allowed the deletion of variables  $T_4(L)$  and  $T_4(0)$ . Eleven equations remained.

Mark 22

This assembly was different from the others in that the outermost annulus was isolated from the three inner annuli. No effective large-scale convection loop could form. Therefore, heat transfer in this assembly was solved by a simple and conservative method. The three outer annuli were assumed to be closed at the top and bottom. A closed convection cell formed in each annulus. The temperature difference across each annulus was calculated with equation

32. The temperature of the hottest surface, the inner fuel tube, was calculated

$$T_{\max} = \bar{T}_S + \Delta T_A + \Delta T_B + \Delta T_C$$

### Results of calculations

The most important result of the calculations was the maximum moderator temperature in the assembly. The difference between the maximum temperature and the tank temperature is plotted versus power in Figures 11, 12, and 13. Tank temperature appears as a parameter.

### CORRECTION FOR NON-UNIFORM HEAT GENERATION ALONG LENGTH OF ASSEMBLIES

The experimental electrically-heated target columns produced heat uniformly along their lengths. Therefore, the analysis assumed a uniform heat production. In reality, the heat production in a reactor assembly is non-uniform. A common power shape has been a flattened cosine curve. The correction of the limit from an assembly with a uniform heat production to one with a flattened cosine power shape involved five steps. First, it was assumed that the convective velocity was unchanged by the change in the power shape. Second, temperatures in the annuli and at the target column surfaces were calculated as non-linear functions of height. Third, the hottest surface temperatures were located. Unlike the uniform power case in which the hottest surface temperature was at the top, the maximum temperature for the flattened cosine case was about two feet from the top. Fourth, assembly power limits were based on the temperature calculations. Fifth, the new convective velocity was calculated. The average temperature difference between the two columns was proportional to density difference and hence to convective velocity. The new convective velocity was higher than the original velocity. For the assemblies in question, increased convective velocity had the effect of enhancing heat transfer. Because the calculation of the assembly power limit used the original velocity, the calculation was conservative.

The steps in the correction process will be given in more detail. The power shape  $P(Z)$ , for the calculation is given in Table III. The fraction of the target column heat going

to the inner and outer surfaces was different at the top and bottom of the column according to the original calculation. A factor J was defined as the ratio of the heat flux at the top of the inner surface of the column divided by the average of the heat fluxes for the top and bottom of the inner surface. For surface 3 J is:

$$J = \frac{2q_3(L)}{q_3(L) + q_3(0)} \quad [42]$$

$$J = \frac{2h_3 [T_3(L) - T_B(L)]}{h_3 [T_3(L) + T_3(0) - T_B(L) - T(0)]} \quad [43]$$

The factor J was evaluated from temperature data. The average of the heat fluxes at the top and bottom of the surface was approximately equal to the average heat flux.

$$\frac{q_3(L) + q_3(0)}{2} = \frac{Q_3}{A_3} \quad [44]$$

Substituting equation 44 into 42 and rearranging gives:

$$q_3(L) = \frac{Q_3 J}{A_3}$$

This equation was generalized to all heights, z.

$$q_3(z) = \frac{Q_3}{A_3} \left[ 1 + (J-1) \left( z - \frac{L}{2} \right) \right]$$

For the non-uniform power shape case the local heat flux was assumed proportional to the local value of the power shape.

$$q_3(z) = \frac{Q_3 P(z)}{A_3} \left[ 1 + (J-1) \left( z - \frac{L}{2} \right) \right]$$

The temperature distribution in annulus B was stepped off with the equation

$$\Delta T_B = \frac{q_3(z) \Delta z}{U_B A_B \rho C_p}$$

The temperature at surface 3 was calculated with

$$T_3(z) = T_B(z) + \frac{q_3(z)}{h_3}$$

These equations were implemented by the computer program SHAPE, listed in Appendix C. The program calculated maximum metal temperatures for each type of assembly. A plot of metal temperature versus power was drawn on log-log paper for each assembly type and moderator temperature. The plots are shown in Figure 14 and 15. Limits were found at the intersection of the plotted curves and lines for temperatures of 100°C and 106°C.

Verification of the power shape correction method assumed that the convective velocity was unchanged. This assumption

was checked for conservatism. The temperature profile in annulus C was calculated. The local heat loss from the annulus was approximately equal to the difference between the local annulus temperature  $T_C(z)$  and  $T_w$ . The heat gain was found by difference knowing the total heat production in the outer target column and the fraction going to annulus B. The local heat flux at surface 5 is

$$q_5(z) = k_1 (T_C(z) - T_w)$$

where  $k_1$  is a constant evaluated such that

$$2\pi r \int_0^L q_5(z) dz = Q_5$$

The heat flux at surface 4 was found from

$$q_4(z) = \frac{Q_T P(z)/L - q_3(z) 2\pi r_3}{2\pi r_4}$$

The temperature distribution in annulus C was stepped off with the equation

$$\Delta T_c = \frac{1}{u_c A_c \rho C_p} [k_1 (T_c(z) - T_w) r_5 - q_4(z) r_4] 2\pi \Delta z$$

The average temperatures in annuli B and C were computed. Equations 2, 4, and 6 were used to compute  $U_B$ . The new value of  $U_B$  was larger than the original value. It was known that larger convective velocities improved the heat transfer process. That implied that the power shape correction method was conservative. The computer program SHP31B did the preceding computation. It is listed in Appendix D.

#### CALCULATION OF POWER LIMITS

Figures 5 and 6 compare the measured maximum temperatures in the test assemblies with the values calculated by the computer model. Considering the complexity of the model and the fact that no adjustable constants were used the agreement is excellent. The discrepancies that exist have two sources, random error and systematic error. Random error results from uncertainties in experimental measurements. If an experiment is repeated the measured values will vary somewhat. The effective magnitude of the random error was found by first adjusting the data to account for the fact that experiments were run at moderator temperatures other than the two nominal temperatures, 30°C and 50°. Because the experimental temperature usually plotted along a straight line on log-log paper, the

dependence of  $(T_3 - T_w)$  on  $T_w$  was assumed to be of the form

$$\frac{(T_3(L) - T_w)_{T_w = T}}{(T_3(L) - T_w)_{T_w = T_{nom}}} = \exp[S(T_{nom} - T)]$$

The constant  $S$  was evaluated with data at moderator temperatures of  $30^\circ$  and  $50^\circ\text{C}$ .

$$\frac{(T_3(L) - T_w)_{T_w = 50^\circ}}{(T_3(L) - T_w)_{T_w = 30^\circ}} = \exp[-20 S]$$

or

$$S = .05 \ln \frac{(T_3(L) - T_w)_{T_w = 30^\circ}}{(T_3(L) - T_w)_{T_w = 50^\circ}}$$

After adjustment to one of the two nominal temperatures the data was plotted on log-log paper and a straight line fitted through each data set.

The deviation of each data point was measured and then a standard deviation was calculated. The deviation tended to be largest for the earliest data taken and improved as experimental procedures were refined. The overall standard deviation (neglecting some early data points with large deviations) was 4.4%.

Next the systematic error was noted. In two cases the computer model systematically underpredicted the maximum metal temperature (either  $T_1$  or  $T_3$  depending on assembly type) by 3%. In the other six cases there was either no systematic error or the model overpredicted the maximum temperature. At worst the overprediction was 20%. The maximum likely systematic error was taken to be 3%.

The temperature limits were calculated in a series of steps. The computer model was run for the Mark 31A, 31B, 16, 16B, 15, and 53A assemblies. Heavy water properties were used. The maximum assembly temperature referenced to tank water temperature was plotted as a function of power on log-log paper, as shown in Figures 14, 15, and 16. The data points appeared to fall on straight lines. Next a parallel line was drawn 16.2% higher to account for the maximum likely systematic error (3%) plus three times the standard deviation of the random error ( $3 \times 4.4\%$ ). Three standard deviations provided a margin of certainty of 99.9%. The 16.2% margin was applied to the curves for the Mark 31A, 31B, 16, 16B and 53A assemblies. The calculation for the Mark 22 assembly was judged to be

simpler and involved less uncertainty. A margin of 10% was used for the Mark 22. The calculated forced cooling limits are in Table I. They are a function of moderator temperature. The highest temperature measured by the moderator thermocouples anywhere in the reactor should be used for  $T_{mod}$ . It is advisable to interpolate between the temperatures listed in the figure. After Technical Specification 105-2.7 has been changed, the limits corresponding to a temperature limit of 106°C should be used. The powers in the figure refer to sensible heat only, not radiation that escapes the assembly without heating it.

The power limits for all assemblies except the Mark 22 were similar; this was because all of the assemblies except the Mark 22 had identical outer annuli. Therefore, heat transfer coefficients across the outer annulus were nearly the same. Also, the contribution of the outer annulus to total flow resistance was the same.

JLS:prc

REFERENCES

1. DuPont Engineering Dept. Design Standards, DG 50C (1981).
2. R. B. Bird, W. E. Steward and E. N. Lightfoot, Transport Phenomena (1960).
3. DuPont Engineering Dept. Design Standards, DG 51C, (1976).
4. J. N. Arnold, I. Catton, and K. D. Edwards, "Experimental Investigation of Natural Convection in Inclined Rectangular Regions of Differing Aspect Ratios", J. Heat Transfer 98 67 (1976).

23  
TABLE I

FORCED COOLING LIMITS BASED ON FLATTENED COSINE POWER PROFILE  
Based on D<sub>2</sub>O properties. Power refers to sensible heat.

Mark 31A	T <sub>mod</sub> °C	Temp. Limit	
		100 °C	106 °C
	30 °C	19.0 kw	21.7 kw
	40	17.0	19.5
	50	14.7	17.5

Mark 31B	Temp. Limit	100	106
		100 °C	106 °C
	30	21.2 kw	24 kw
	40	18.0	20.8
	50	15.2	18.0

Mark 16-16B	Temp. Limit	100	106
		100 °C	106 °C
	30	20.0 kw	22.2 kw
	40	17.2	19.6
	50	15.0	17.4

Mark 53A	Temp. Limit	100	106
		100 °C	106 °C
	30	24.0 kw	27.2 kw
	40	20.7	24.0
	50	17.0	20.0

Mark 22	Temp. Limit	100	106
		100 °C	106 °C
	30	11 kw	12.5 kw
	40	9.4	10.5
	50	7.7	9.0

Mark 15	Temp. Limit	100	106
		100 °C	106 °C
	30	20.0 kw	23.0 kw
	40	18.3	21.0
	50	14.5	17.5

TABLE I (Cont.)

OX2	$T_{mod}$	Temp. Limit	$100^{\circ}C$	$106^{\circ}C$
.	$30^{\circ}C$		21.0 kw	24.5 kw
.	$40^{\circ}C$		19.5	22.5
.	$50^{\circ}C$		16.0	19.3

TABLE IIREACTOR ASSEMBLY DIMENSIONS

	<u>r<sub>o</sub></u> , ft.	<u>r<sub>i</sub></u> , ft.
USH	.1713	.1671
Mark 31A outer target	.1542	.1079
inner target	.0925	.0521
inner housing	.0417	
Mark 31B target	.1542	.1079
inner housing	.0938	
Mark 16-16B outer fuel	.1542	.1431
middle fuel	.1223	.1079
inner fuel	.0868	.0716
inner housing	.0574	
Mark 22 outer target	.1542	.1475
outer fuel	.1333	.1205
inner fuel	.0980	.0831
inner target	.0663	
Mark 53A target	.1542	.1365
inner housing	.1243	

TABLE III

FLATTENED COSINE FLUX SHAPE

Nondimensional

top	.351
	.460
	.782
	.959
	1.100
	1.205
	1.265
	1.290
	1.300
	1.300
	1.300
	1.300
	1.290
	1.265
	1.215
	1.152
	1.075
	.957
	.807
bottom	.630

Figure 1

Mark 31A Assembly

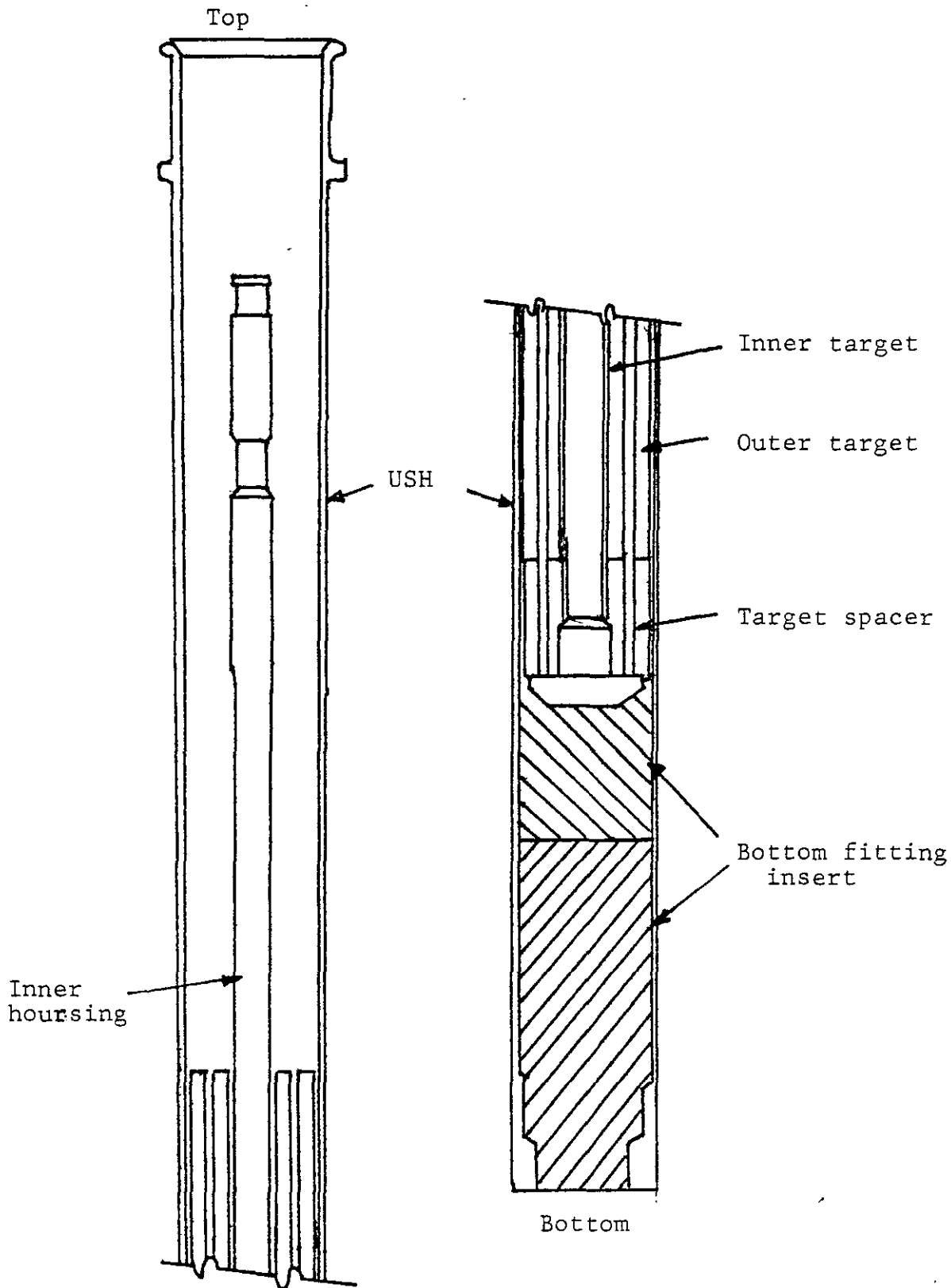


Figure 2  
Conductivity Probe Circuit

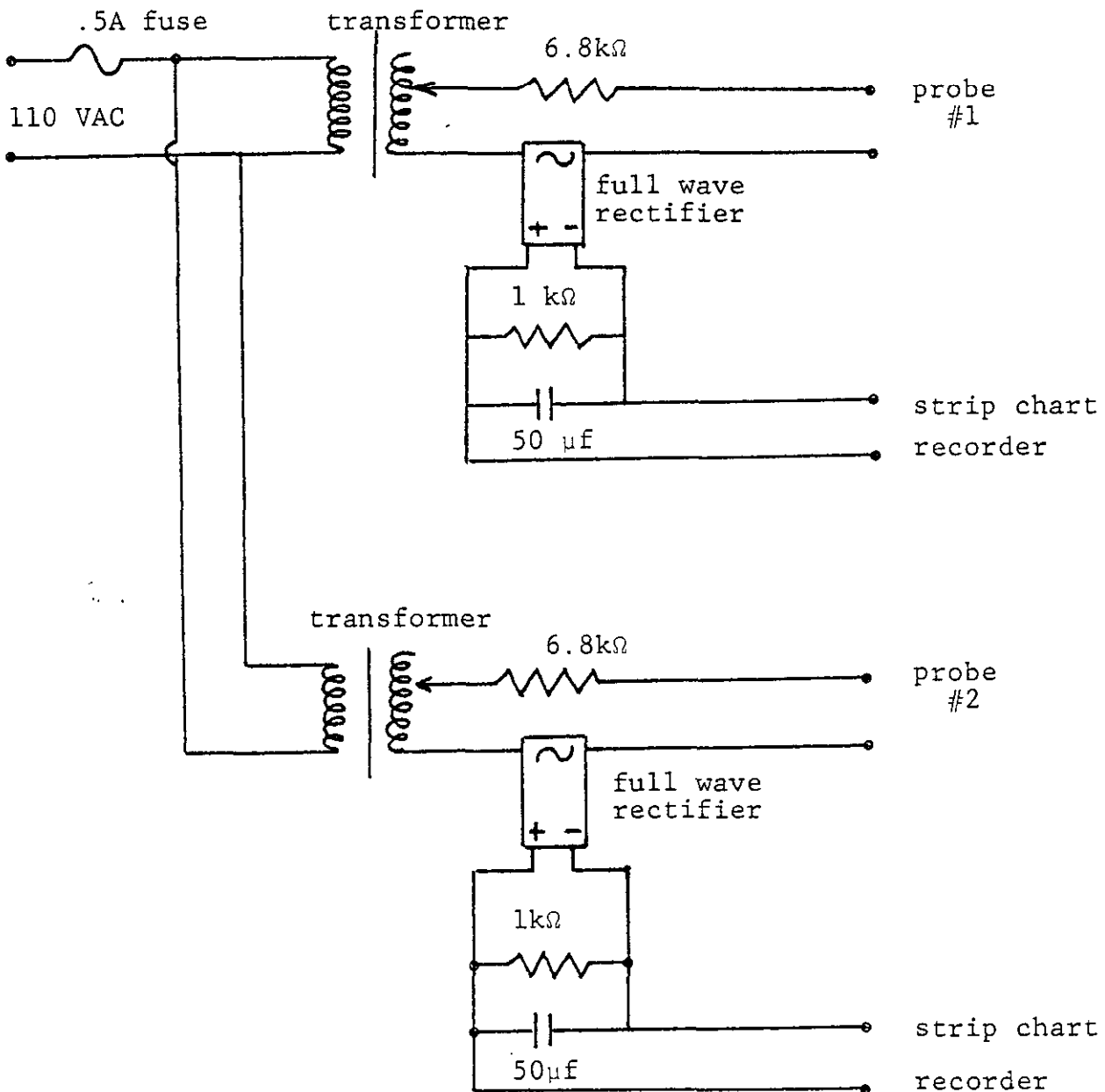


Figure 3  
Velocity Measurement

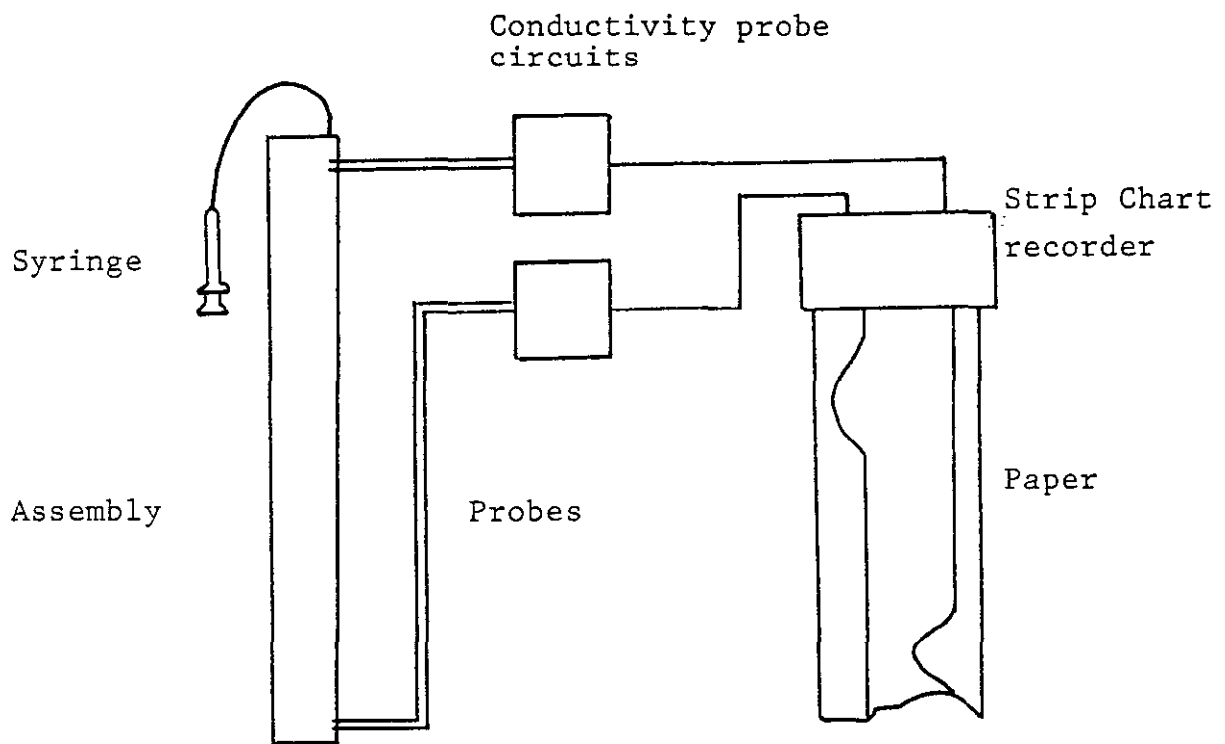


Figure 4  
Model of Mark 31A Assembly

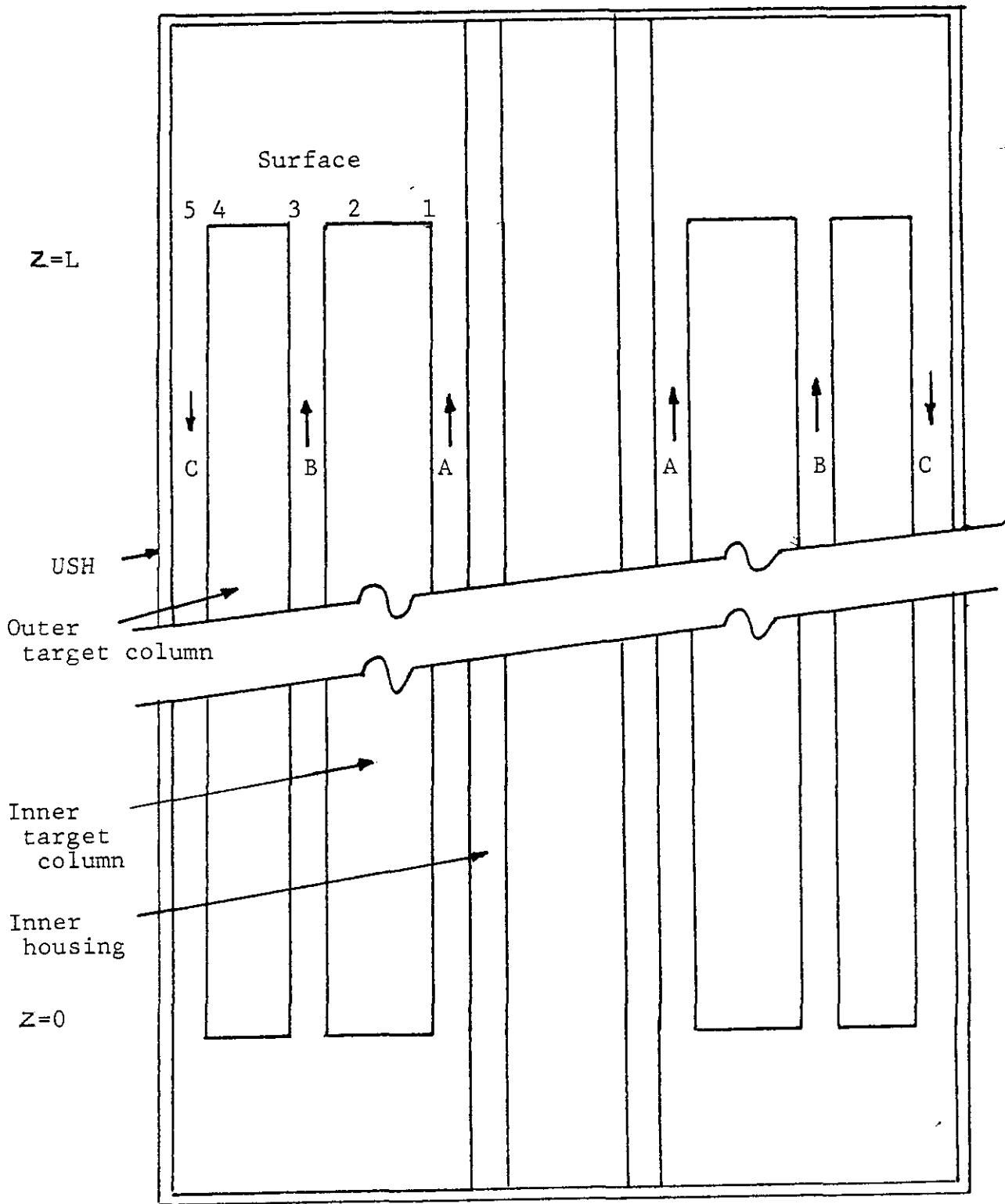


FIGURE 5

HOTTEST ASSEMBLY TEMPERATURE, SURFACE 1 AT TOP, MARK 31A

Curves are results of computer model

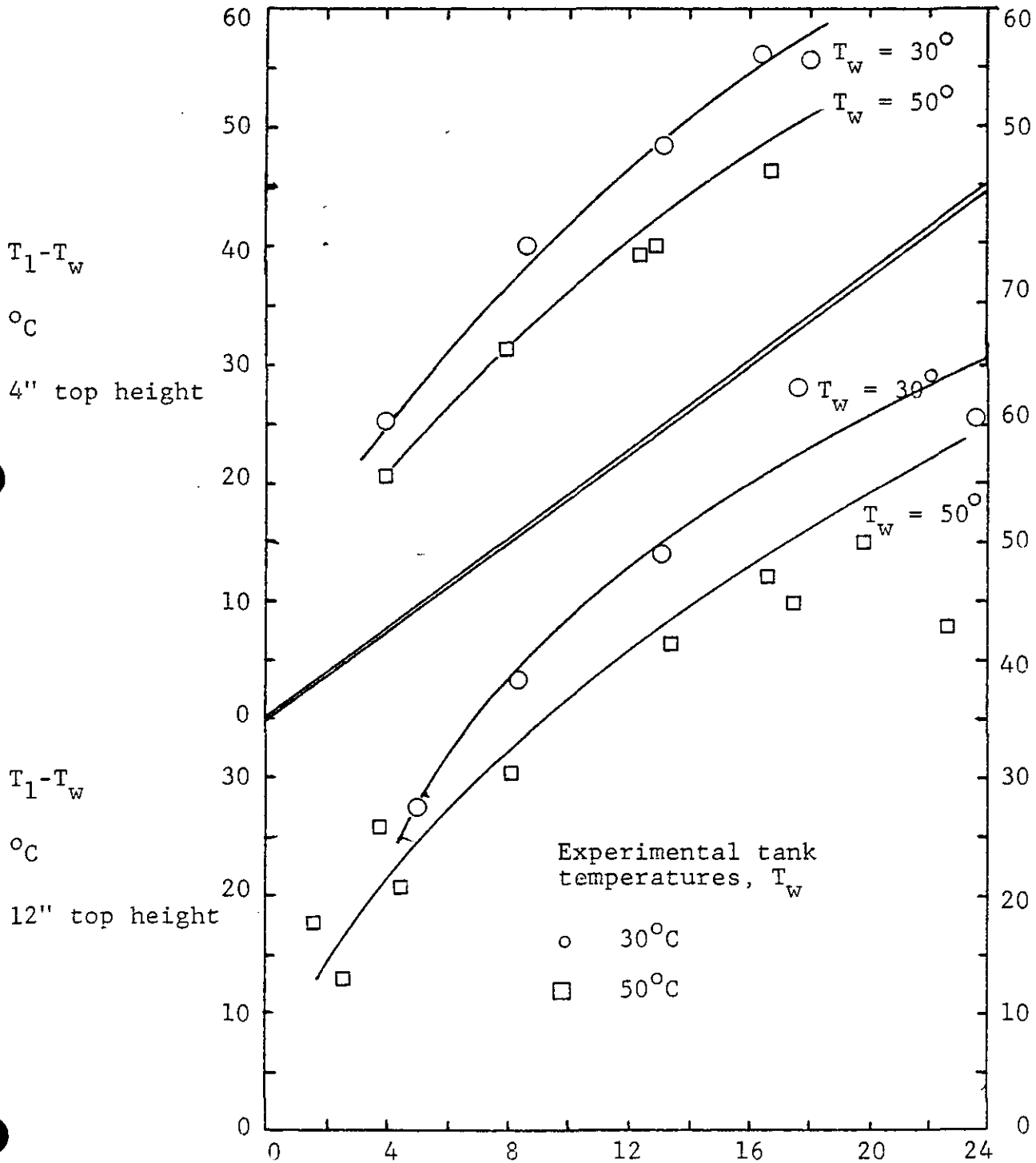


Figure 6

Hottest Assembly Temperature, Surface 3 at Top, Mark 31B

Curves are results of computer model

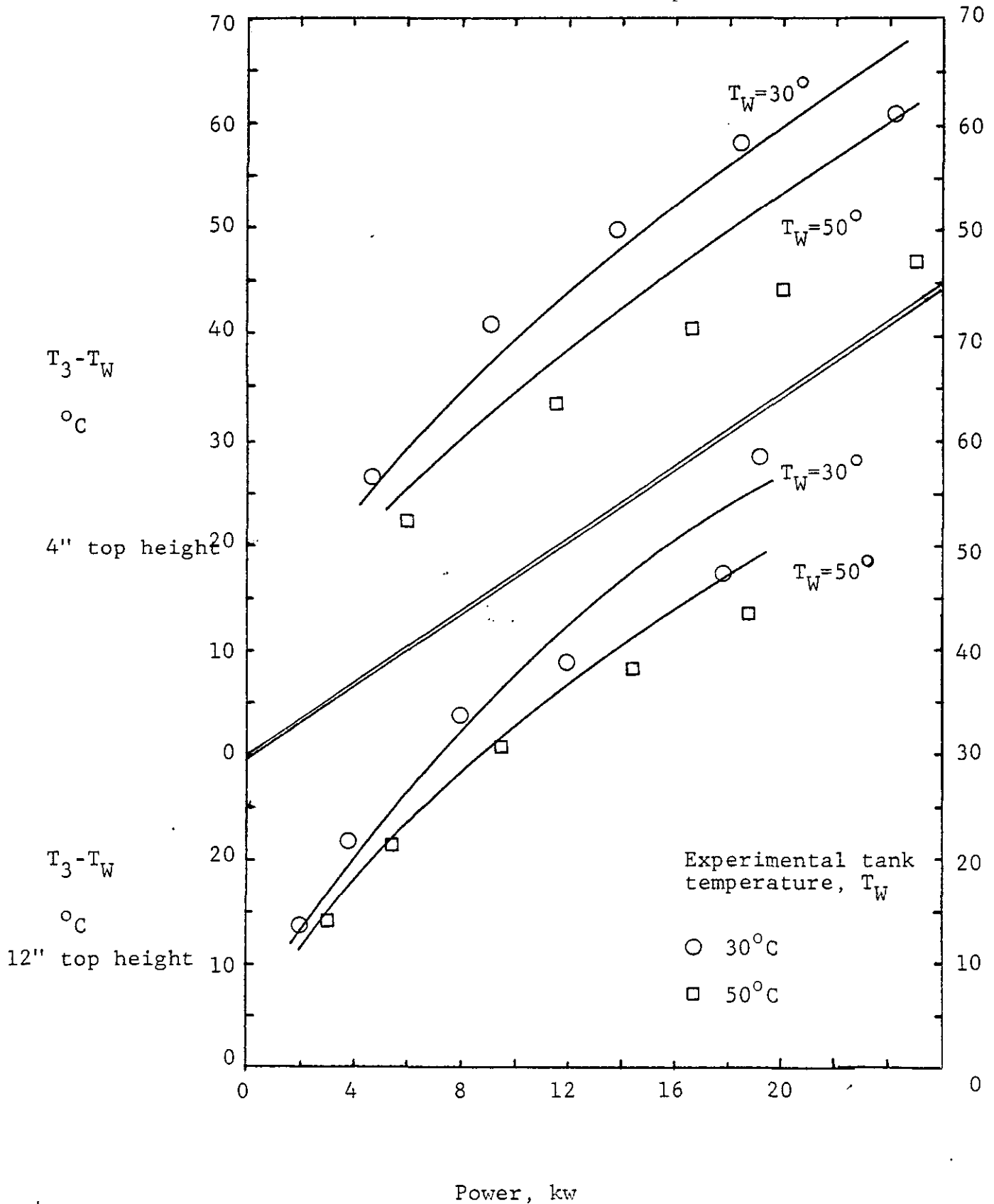


Figure 7  
Outer Annulus Temperature at Top, Mark 31A

Curves are results of computer model

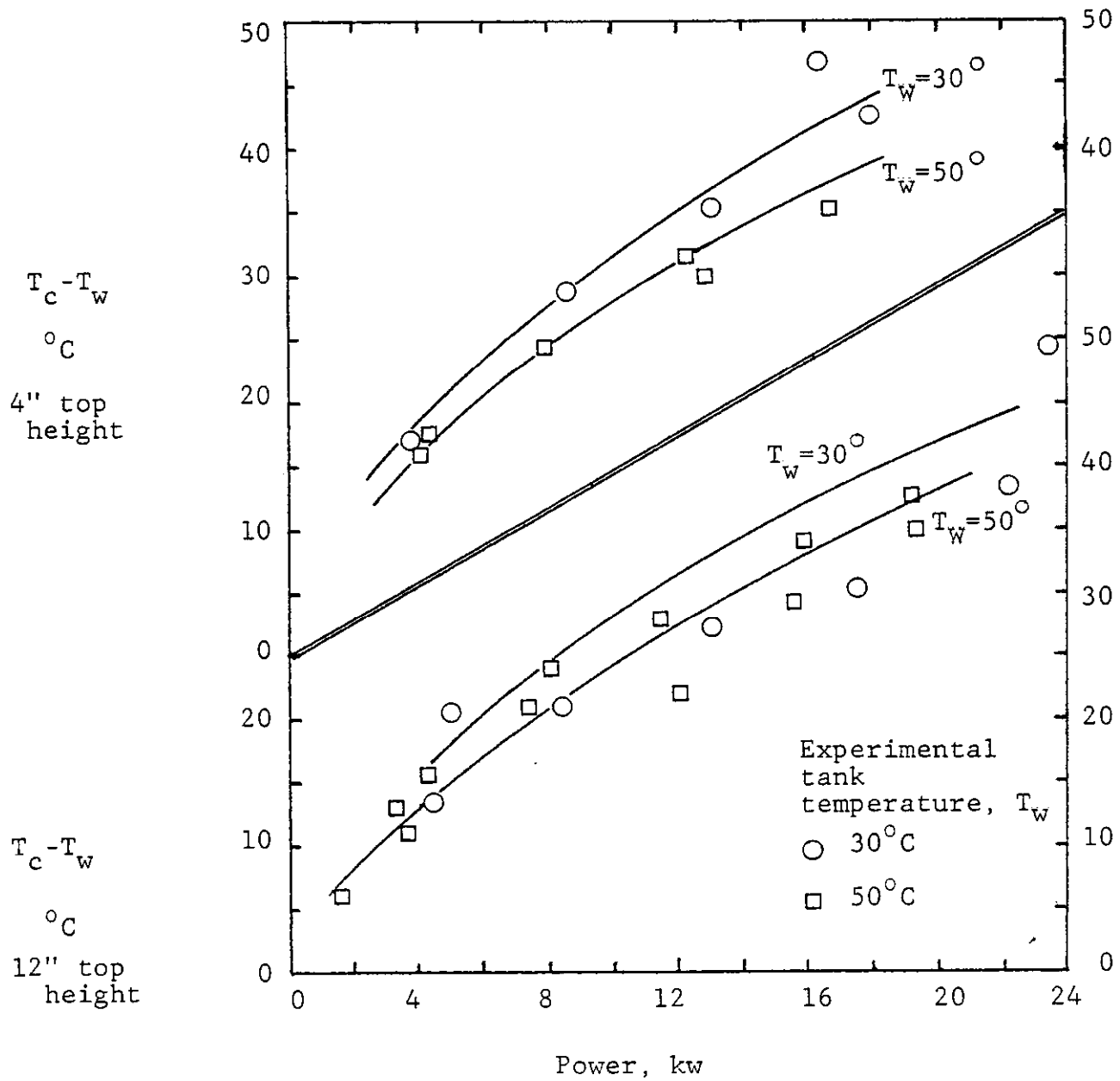


Figure 8  
Outer Annulus Temperature at Top, Mark 31B

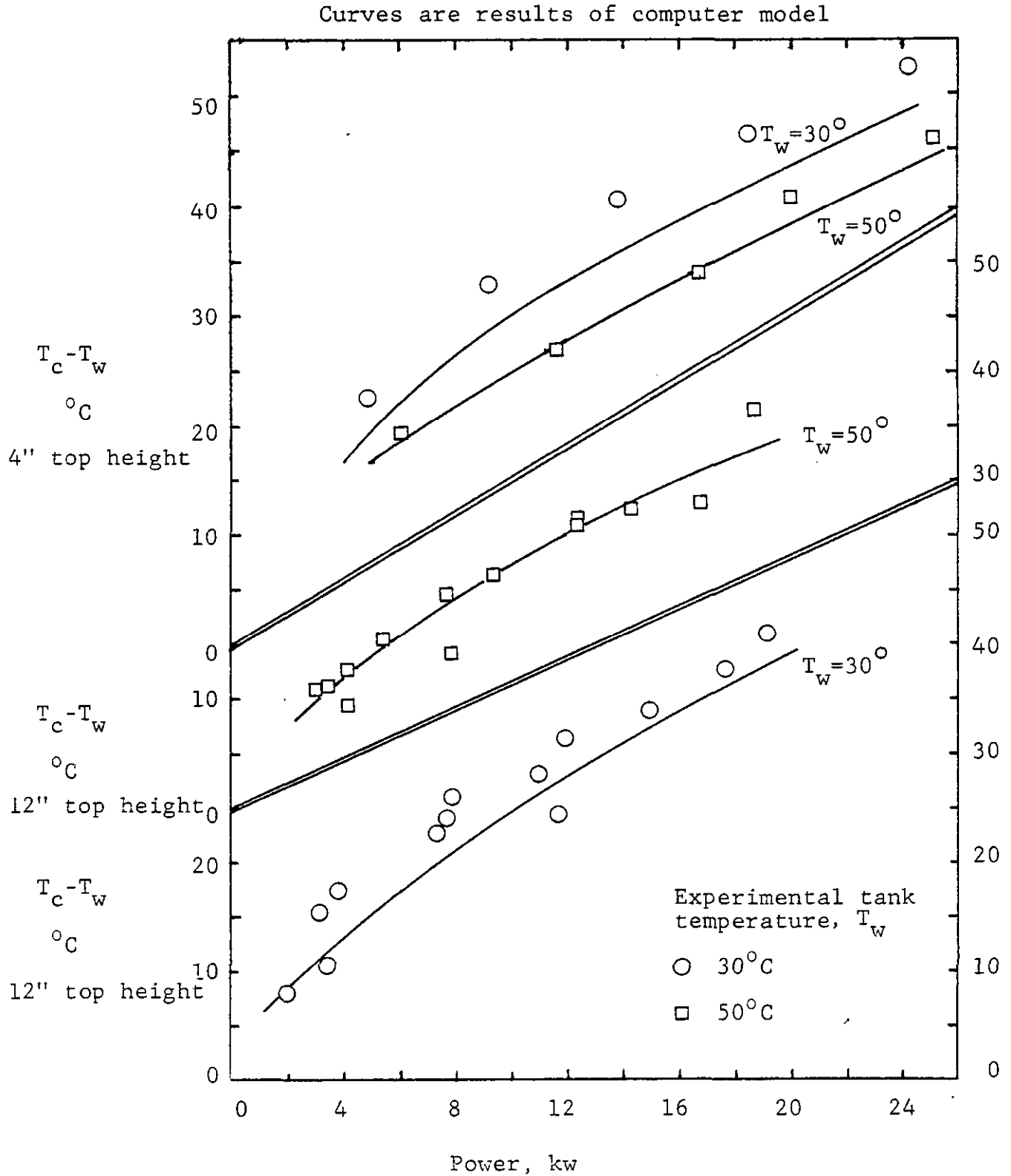


Figure 9  
Annulus B Velocity, Mark 31A

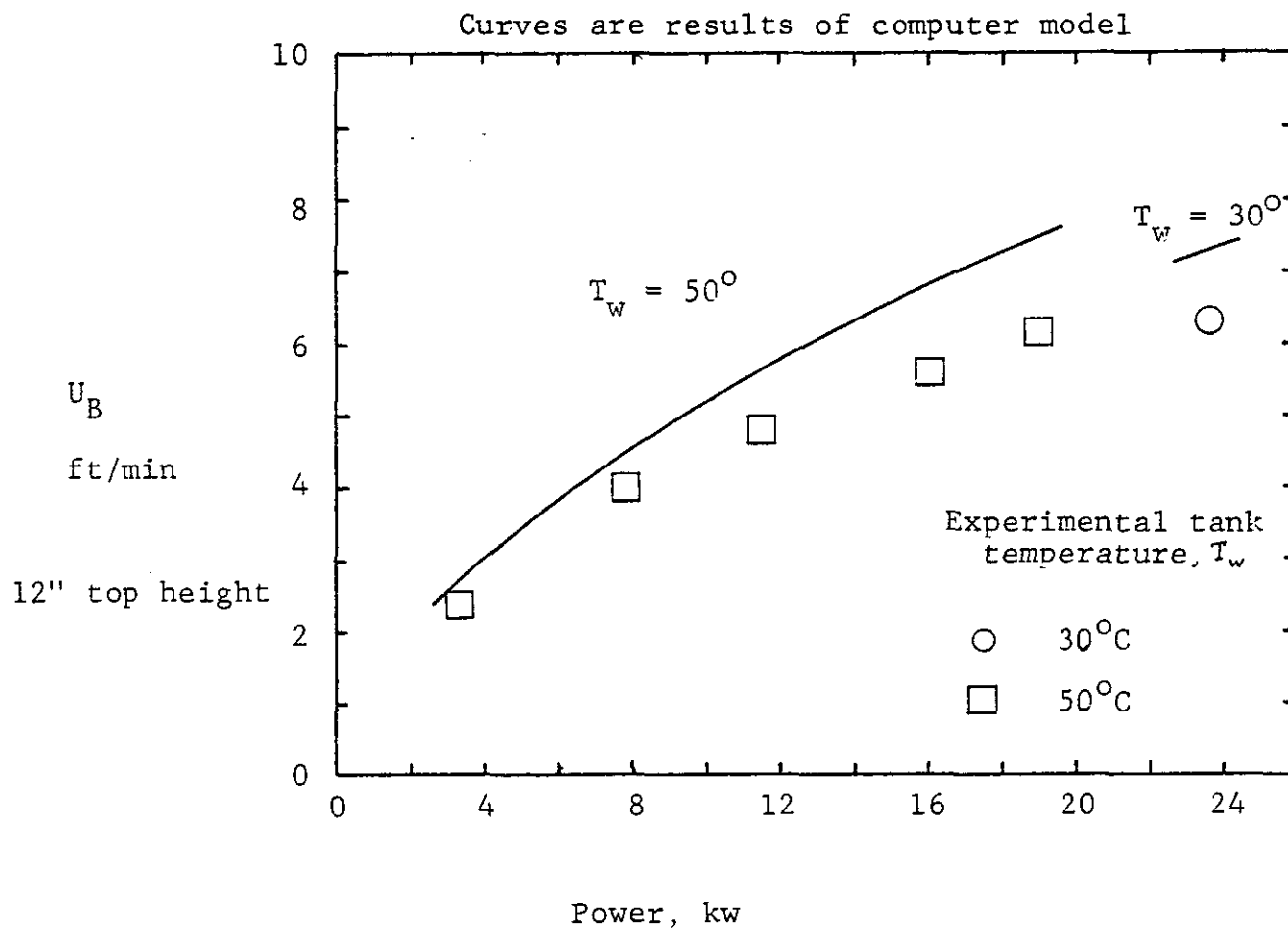


Figure 10  
Annulus B Velocity, Mark 31B

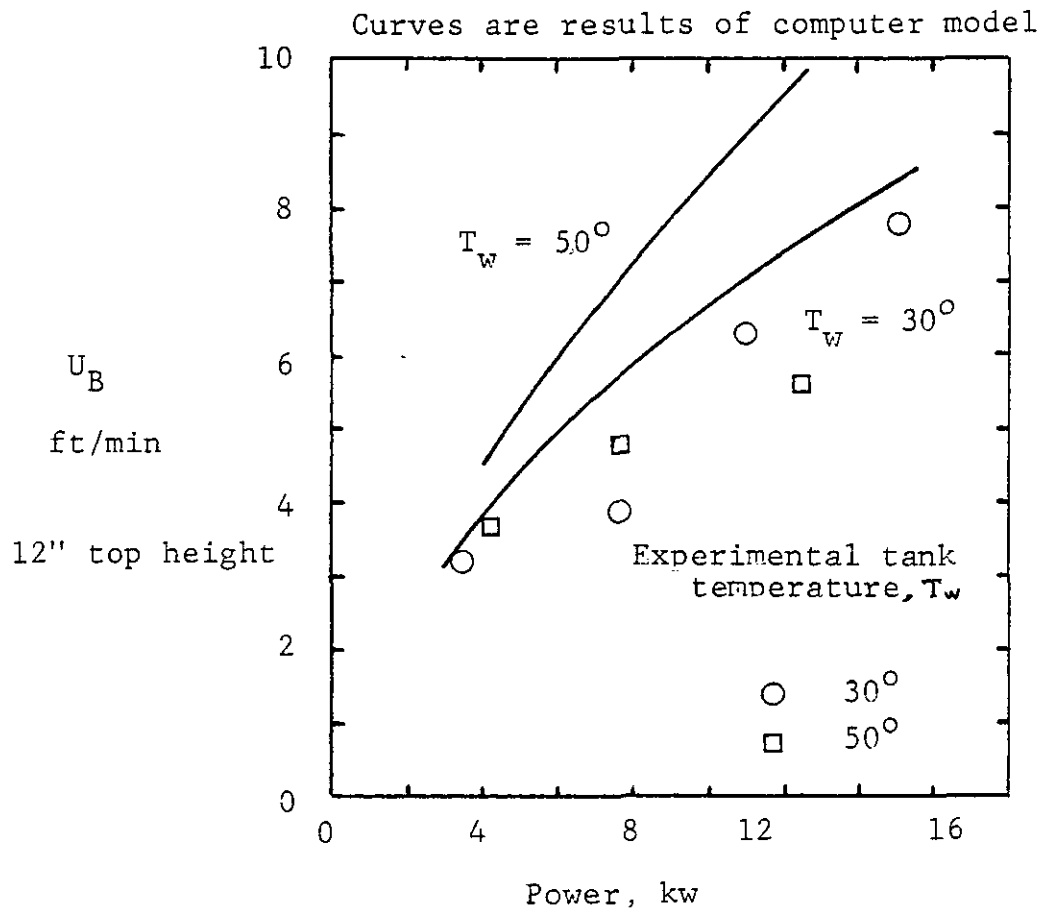


Figure 11

Results of Computer Model Calculation of  
Assembly Maximum Temperature

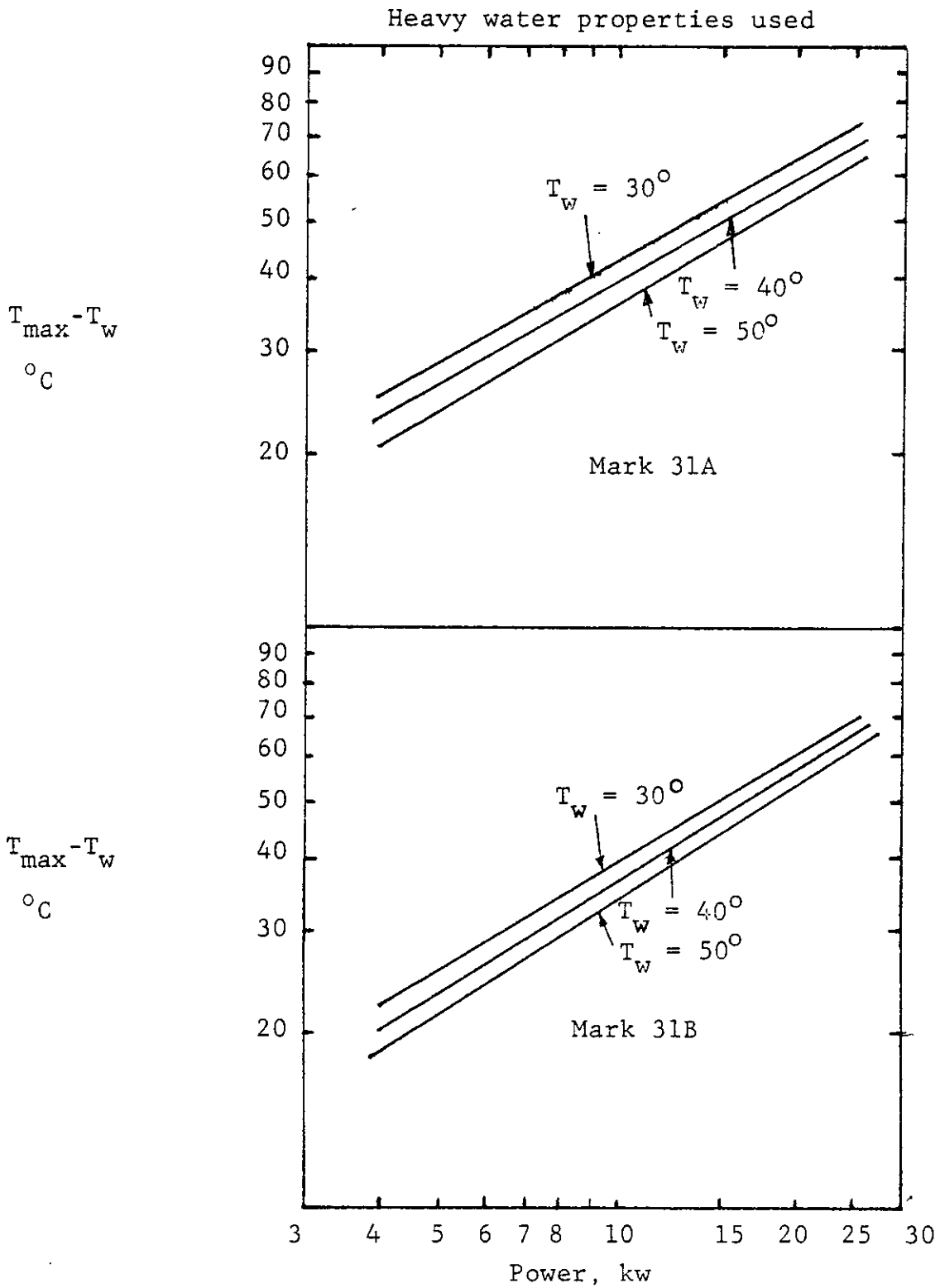


Figure 12  
Results of Computer Model Calculation of  
Assembly Maximum Temperature

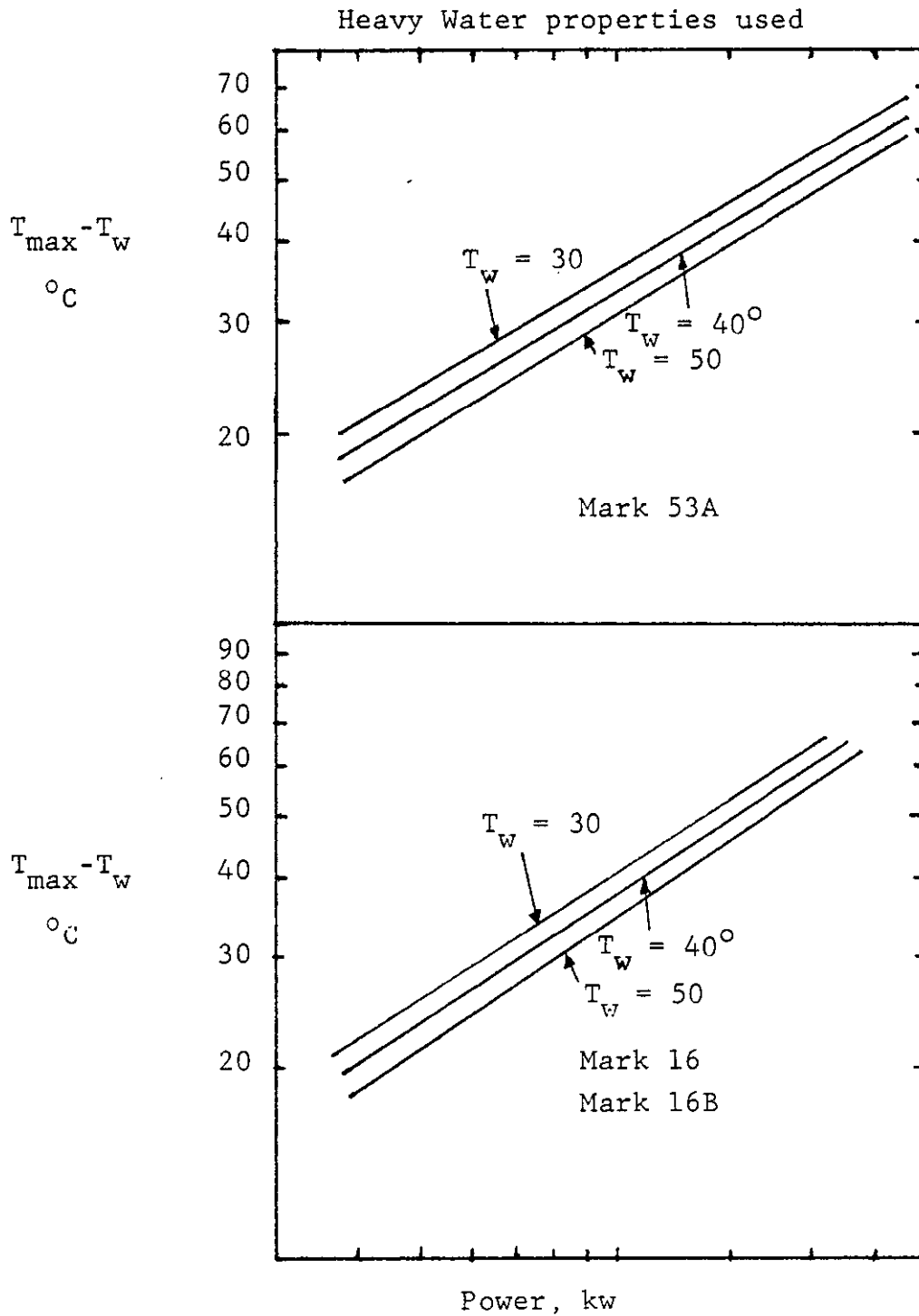


FIGURE 13

Results of Computer Model Calculation of  
Assembly Maximum Temperature

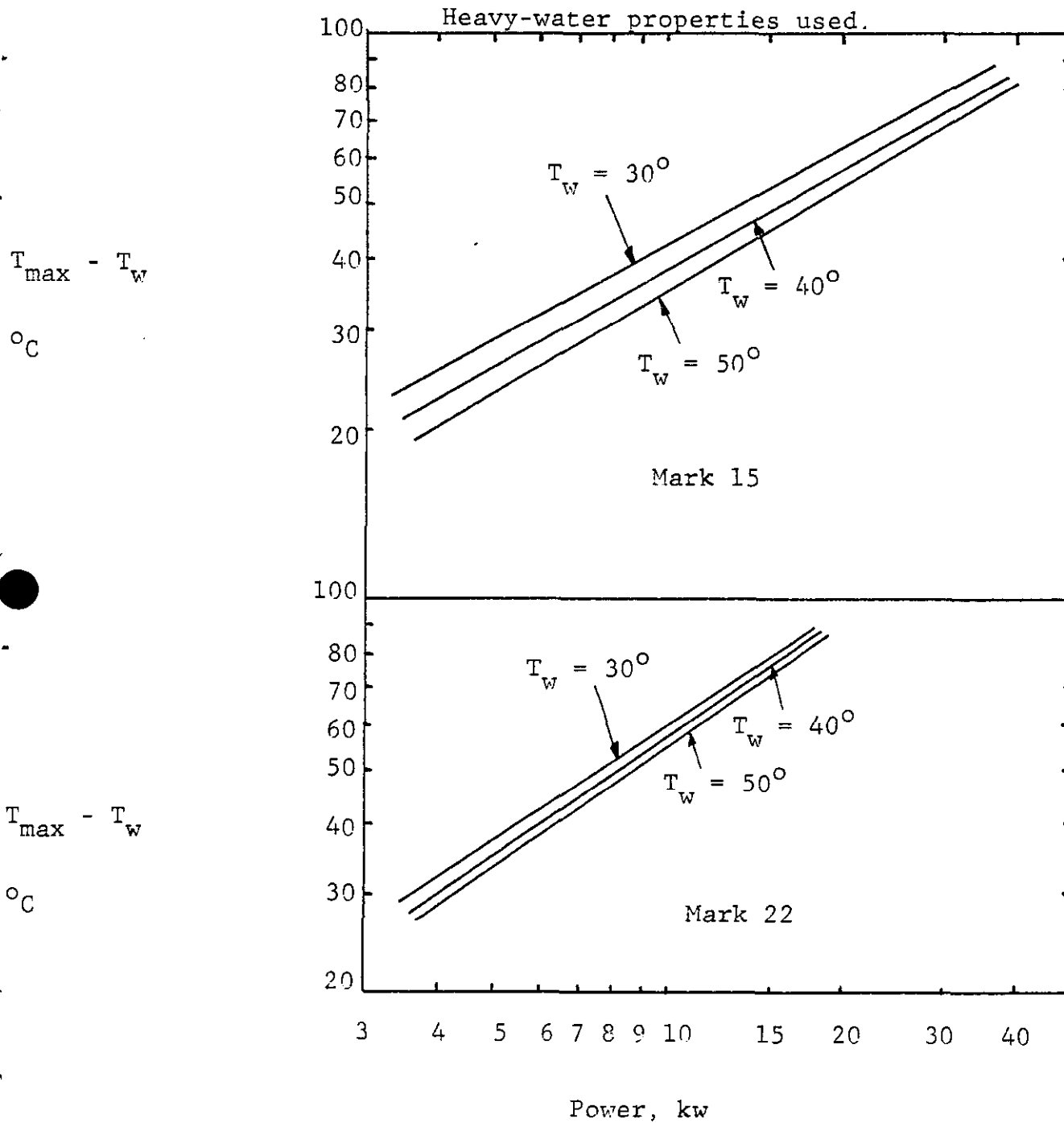


Figure 14

## Graphical Solution for Assembly Power Limits

Solid lines are maximum temperature curves adjusted for non-flat power profile. Dashed curves account for uncertainty.

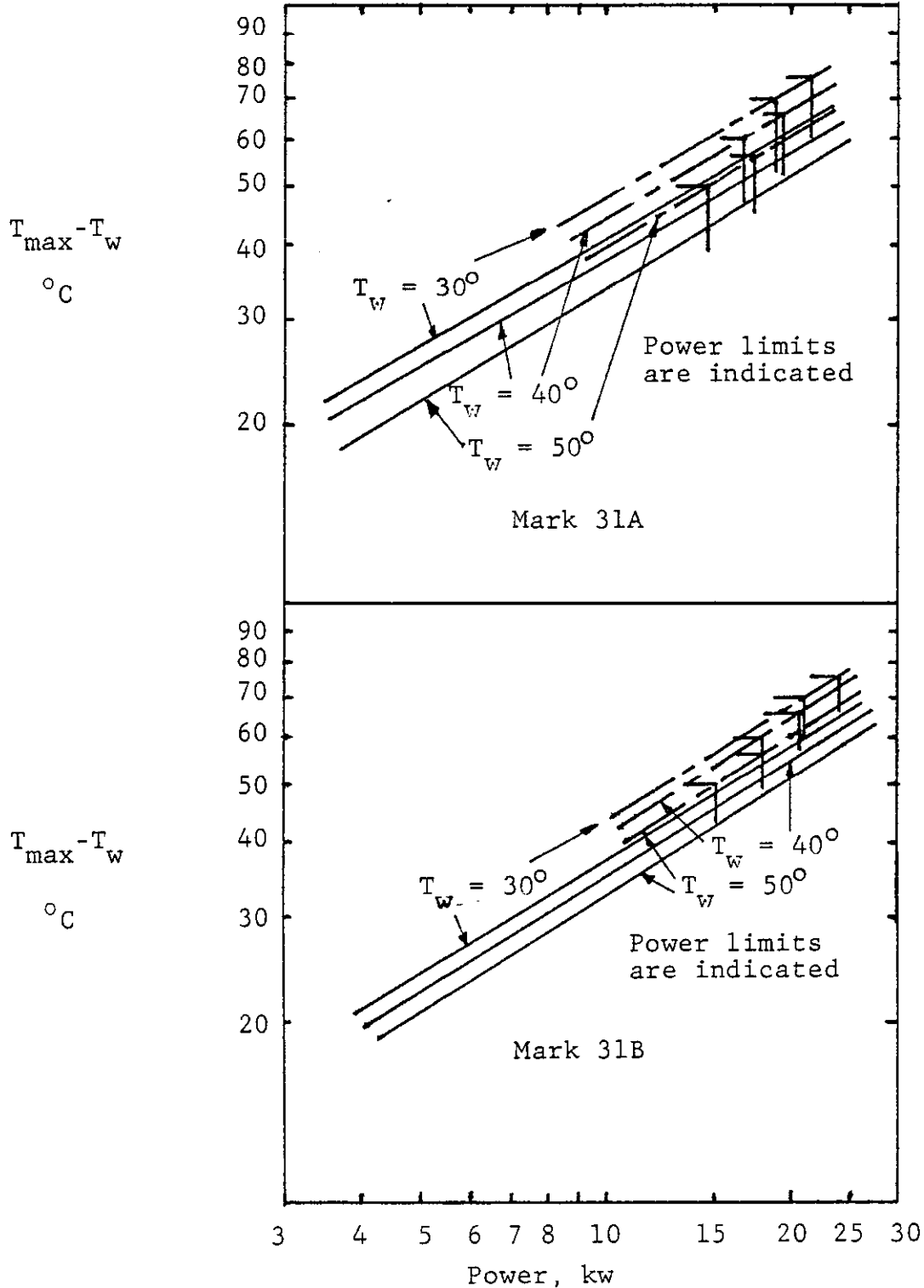


Figure 15

Graphical Solution for Assembly Power Limits

Solid lines are maximum temperature cuves adjusted for non-flat power profile. Dashed curves account for uncertainty.

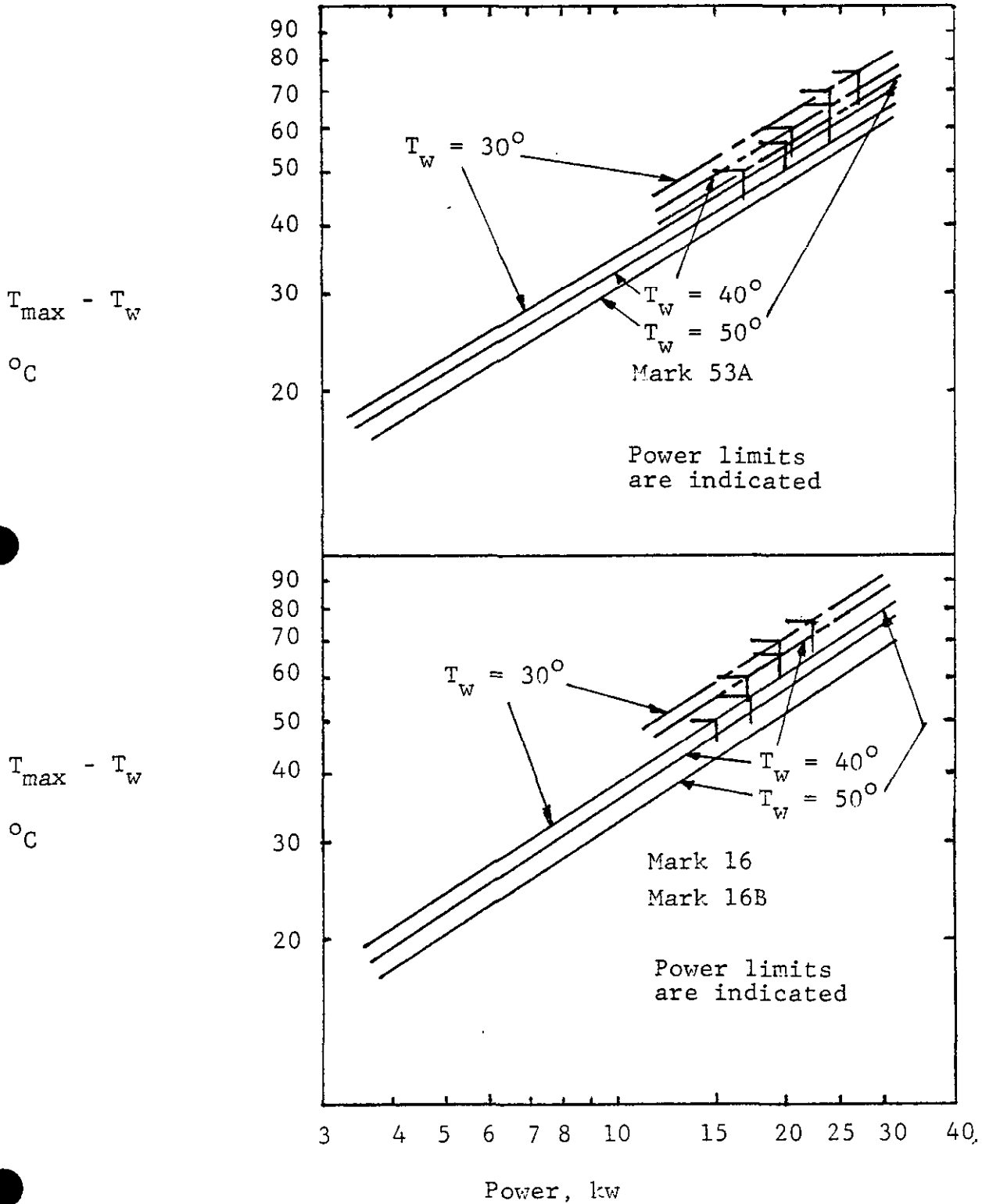
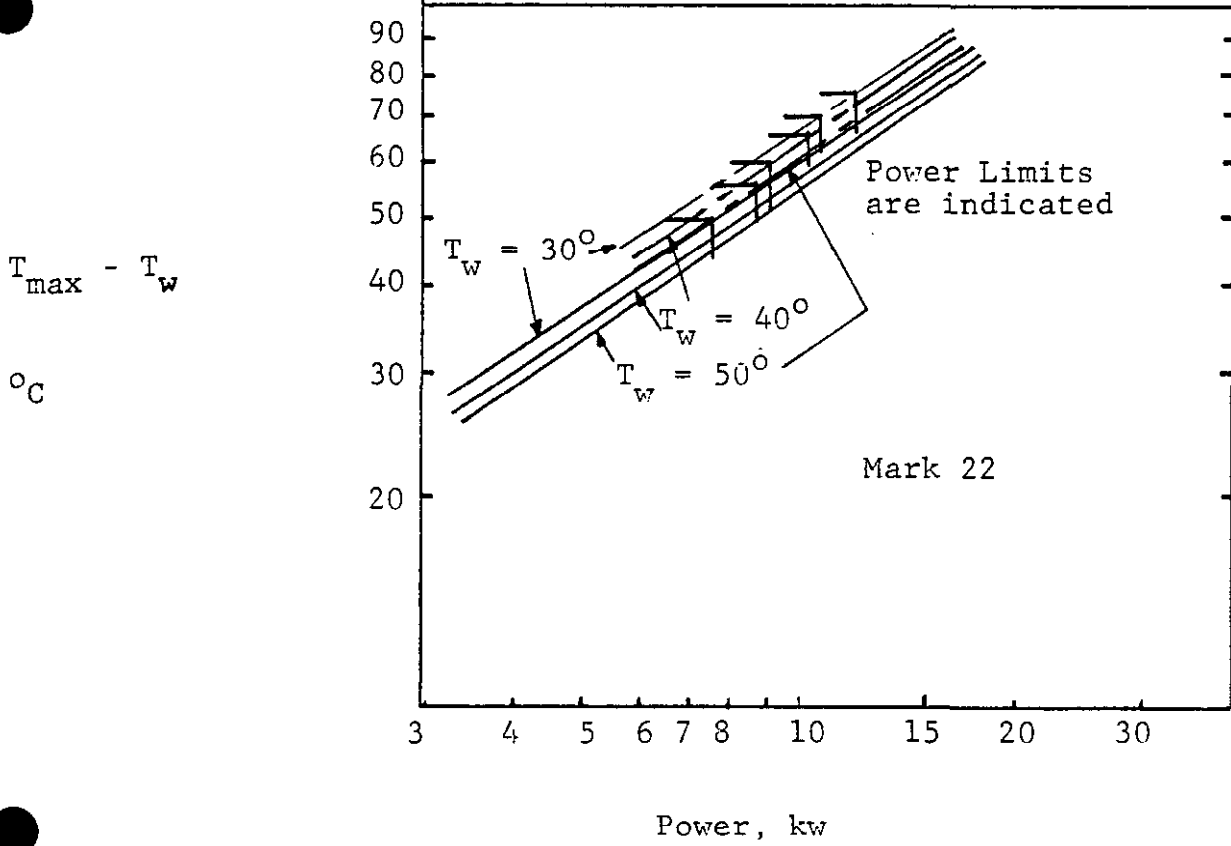
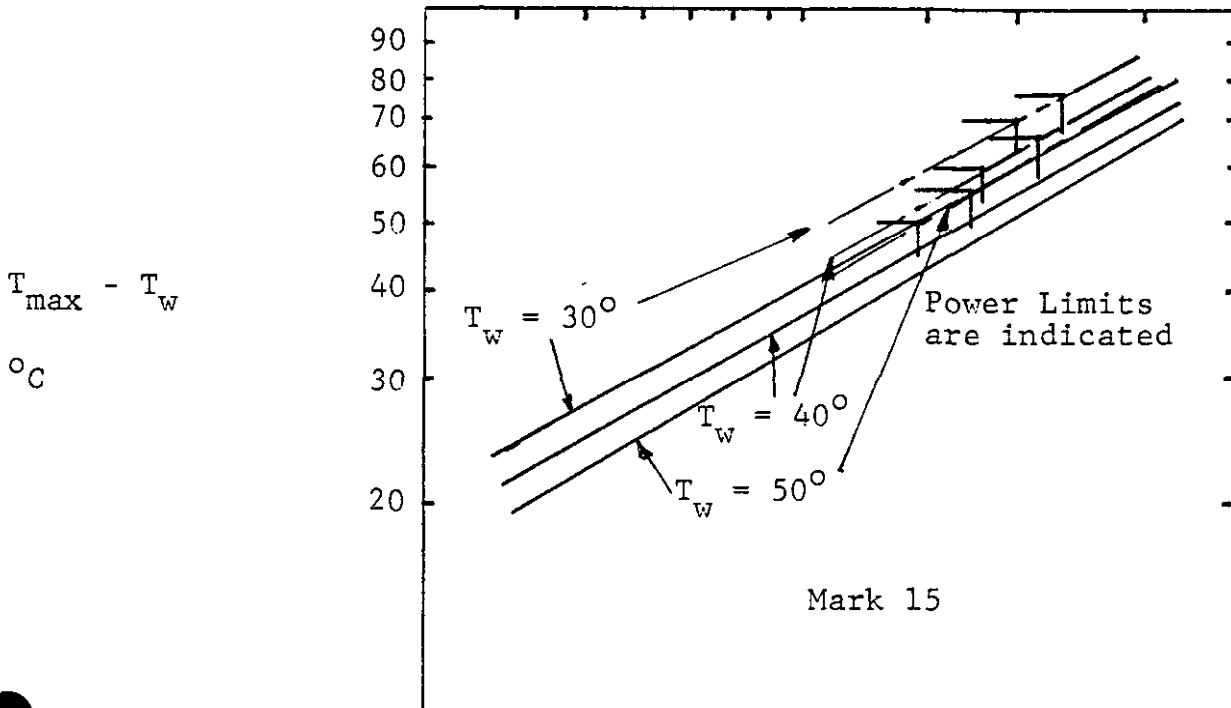


FIGURE 16

Graphical Solution for Assembly Power Limits  
 Solid lines are maximum temperature curves adjusted for non-flat power profile. Dashed curves accounts for uncertainty.



Appendix ACALIBRATION METHODS AND RESULTS

The original data for the calibrations are in notebooks DPSTN-3087 and DPSTN-3282.

Thermocouples

One thermocouple was calibrated by comparison to a precision glass thermometer. A comparison of temperature readings is given below.

<u>Glass Thermometer reading</u>	<u>Thermocouple reading</u>
0.0 °C	0.0
20.5	20.0
40.5	40.0
60.0	60.0
79.7	80.0
99.3	99.5

The maximum discrepancy was .5°C. Also, all of the thermocouples were checked for consistency. A-tank, in 786-A which held the test assembly and eight thermocouples, was filled with water at a uniform temperature. The thermocouple readings are listed as follows:

<u>TC#</u>	<u>Reading (°C)</u>
1	47.4
2	47.3
3	47.3
4	47.5
5	47.3
6	47.5
7	47.5

Table (cont.)

<u>TC#</u>	<u>Reading (°C)</u>
8	47.5
9	47.3
10	47.7
11	47.8

The maximum variation was .5°C.

#### Strip chart recorder

The accuracy of the feed rate of the strip chart recorder determined the accuracy of fluid velocity measurements. The feed rate was timed with a laboratory stopwatch. Accuracy was better than one part in 240.

#### Rectifier voltmeter and current meter

The assembly power was calculated as the product of voltage drop and current. The voltmeter was calibrated with a precision digital voltmeter. The rectifier voltmeter was found to read 8% too high. The experimental readings were corrected accordingly.

Each rectifier had its own current meter. The total current was summed arithmetically. The current meter were calibrated in a flow- $\Delta T$  experiment. The current passed through a brass pipe. The pipe was carefully insulated with foam glass insulation. The water temperature was recorded both entering and leaving the pipe. The flow rate was measured by bucket, stopwatch, and scales. The flow- $\Delta T$  heat rate was compared with the product of current and voltage. During the experiments the flow varied, presumably because of fluctuations in line pressure, and subsequently affected the accuracy of the experiment. Data are given in Table A-I for rectifiers #1 and #3.

The data for currents of approximately 1000 amperes were the least accurate because the temperature increase was only about 3°C. For the other data, any systematic discrepancy between measured electrical power and heat production was not apparent. Random errors were felt to be due to flow variations. The conclusion was to accept the current meter readings at face value.

Velocity measurements

The salt injection method for measuring fluid velocities was checked in two ways. First, a test annulus was constructed. Water flowed up it at a known velocity. Salt solution was injected and the transport time between conductivity probes was recorded. The passage of a salt pulse was not sharply defined because the salt spread axially. The center of the pulse recorded on the strip chart paper was calculated graphically. The following table lists the ratios of measured velocities to actual velocities for the calibration tests.

<u>Velocity (ft/min)</u>	<u>Ratio measured/actual velocity</u>
4.56	.87
11.04	.88
11.04	.87
11.04	1.03
18.78	.91
18.78	.93

The average value of the ratio was .915 with a standard deviation of .06. The raw velocity data was corrected by dividing with a value of .915.

The second check on the salt injection method was the computation of mass balances. The total mass flow rate for the upflow channels should equal the downflow rate in the outer annulus. The following equations for mass balance were used for the Mark 31A and 31B assemblies

$$\begin{aligned} \text{Mark 31A} & \quad .213 V_A + .732 V_B = V_C \\ \text{Mark 31B} & \quad .732 V_B = V_C \end{aligned} \quad (A-1)$$

The ratios between  $V_C$  measured and  $V_C$  calculated with equation (A-1) for several experiments are listed as follows.

Assembly	$V_C$ (meas.) (ft/hr)	$\frac{V_C \text{ calc.}}{V_C \text{ (meas.)}}$
Mark 31A	318	1.01
	357	1.04
	429	.97
	450	1.05
Mark 31B	204	.78
	288	.88
	300	1.04

With the exception of one data point for the Mark 31B all mass balances are within 12% of being correctly conserved.

TABLE A-I  
Current Meter Calibration

Rectifier	Current	$\frac{\text{Power (Volts-Amps)}}{\text{Power (Flow - } \Delta T)}$
#1	1000	.94
	980	.87
	2020	1.06
	2000	.98
	3080	1.03
	3050	.99
	4030	1.05
	4020	1.02
	990	.94
	985	.95
	2000	.98
	2005	.96
	2990	1.02
	2995	1.01
	3990	.99
	3995	.99
	4675	1.02
	4675	1.01
	#3	1005
1010		.84
1998		.95
1995		.92
3000		.93
3000		1.02
4010		.98
4010		1.01
4565		1.00
4565	.98	

## Appendix B

PROPERTIES OF LIGHT AND HEAVY WATER ( $40^{\circ}\text{C} < T < 90^{\circ}\text{C}$ )1. Thermal conductivity, PCU/ $^{\circ}\text{C}$  ft hr

$$\text{H}_2\text{O} : k = .331 + 7.34 \times 10^{-4}T$$

$$\text{D}_2\text{O} : k = .316 + 6.75 \times 10^{-4}T$$

2. Coefficient of thermal expansion,  $(^{\circ}\text{C})^{-1}$ 

$$\text{H}_2\text{O} : \beta = 7.04 \times 10^{-6} + 1.15 \times 10^{-5}T - 4.61 \times 10^{-8}T^2$$

$$\text{D}_2\text{O} : \beta = 7.48 \times 10^{-6}T + .69 \times 10^{-4}$$

3. Viscosity, lb/ft hr

$$\text{H}_2\text{O} : \mu = 2.05 - .0146T$$

$$\text{D}_2\text{O} : \mu = 1.714 \times 10^{-4}T^2 - 4.45 \times 10^{-2}T + 3.52$$

```

C
C PROGRAM MK31AX
C SOLVES HEAT TRANSFER EQUATIONS FOR MK 31A EXPERIMENT
C INPUT UNITS TEMP. (C) POWER (KW)
C FLAG MM=0 FOR 12 TACH TOP SPACE MM=1 FOR 4 TACH
0001      DOUBLE PRECISION A(21,21),P(21),C(21),F,AA(21,21),CC(21)
0002      DIMENSION TAB(3),R(3),U(3),X(3),P(3),GP(3),TX(3),T(3),XP(3),DT(21)
0003      REAL NU(3)
0004      DATA P,X/.0521,.0925,.1079,.0104,2*.0154/
0005      DO 2 I=1,21
0006      2 READ(5,3)(A(I,J),J=1,10)
0007      3 FORMAT(10F7.2)
0008      DO 22 I=1,21
0009      22 READ(5,3)(A(I,J),J=11,20)
0010      DO 23 I=4,21
0011      23 A(I,21)=0.
0012          A(I,21)=-1.
0013          A(2,21)=.00239
0014          A(3,21)=.00239
0015      WRITE(6,6)
0016      6 FORMAT(' INPUT MATRIX')
0017      DO 7 I=1,21
0018      7 WRITE(6,9)(A(I,J),J=1,21)
0019      8 FORMAT(1X,5F5.2,3F4.0,1CF6.0,1X,2F7.5,FP.5)
C INPUT AND EXPERIMENTAL DATA
C VECTOR XP IS TAx, TAx, TCX, T12, T14, TWPX, UAX, UAX, UCX
0020      14 READ(5,1) P,TWC,TWIC,(XP(I),I=1,9),MM
0021      1 FORMAT(11F6.0,FE.0,11)
0022      IF(P .EQ. 0.) GO TO 13
0023      IF(MM .EQ. 0) TCF=1.076
0024      IF(MM .EQ. 1) TCF=.359
0025      RHO=.624
0026      TW=TWC*.8+32.
0027      TWI=TWIC*.8+32.
0028      QB=P/2.93F-4*.731
0029      QI=C0/7.731*.269
0030      TF=TW+10.
0031      K=1
0032      DO 16 I=1,4
0033      7=-.25*TF+15.7
0034      TM=TW+(1.0711*(QI+CC)/Z1)**.75
0035      16 TF=(TW+TM)/2.
C MAKE INITIAL GUESSES OF VARIABLES      TAB IS TA OR TF
C TX IS TB ,ETC.
0036      T5=2.*TM-1k
0037      UB=24.*P+110.
0038      UBB=UB
0039      UC=UB
0040      UA=UB*.5
0041      T45F=(100/37P.1)**.761/2.
0042      TW0=TW+.5.
0043      DO 18 I=1,3
0044      18 TX(I)=TW0+T45F/2.
0045      T1R=TX(1)
0046      T2R=TX(2)
0047      T3R=TX(3)

```

```

0049 1A=15+1450*2.
004C 10=1A
0050 1C=15+145R
0051 11=1A*1.
0052 12=11
0053 13=11
0054 14=11
0055 C5=100+011+.9
0056 90 17 1=1.21
0057 17 A(1)=0.
0058 R(5)=Q5
0059 A(6)=1A
0060 A(7)=1R
0061 A(8)=1C
0062 A(9)=11
0063 A(10)=12
0064 B(11)=13
0065 A(12)=14
0066 B(13)=15
0067 B(14)=11R
0068 A(15)=12R
0069 A(16)=13R
0070 A(18)=12D
0071 A(19)=0A
0072 A(20)=UR
0073 A(21)=UC
0074 N=21
0075 NN=21
0076 JJ=0
0077 WRITE(6,4)
0078 4  FORMAT(//,6X,'PCWER',5X,'Q01',8X,'OF',8X,'16C',7X,'14C',6X,'18',
      *8X,'14T',7X,'1F',8X,'1M',4X,'1CP')
      *R(1),6,5) P,CC,CJ,16C,16T,1K,14T,1F,1M,1CP
0079 5  FORMAT(1X,9F10.1,F10.3)
      *R(1),6,9)
0080 9  FORMAT(//,5X,'C3',5X,'C4',5X,'Q5',6X,'1A',6X,'1B',
      *4X,'1C',4X,'11',6X,'12',6X,'13',6X,'14',6X,'15',6X,'16',6X,'17',6X,'18',6X,'19',
      *12R',3X,'13R',2X,'14R',3X,'16R',3X,'18R',3X,'19R',4X,'UR',4X,'UC')
0081 WRITE(6,10)(P(1),I=3,21)
0082 10 60 KK=1,20
0083 IF(JJ,60,1) CF TC 65
0084 1V1S=.25*TC+.25*TR+.5*1MB
0085 1V1A=2.*1-6*1V1S
0086 1V1S=2.*31-.00R1*1V1S
0087 IF(V1S,11,1) V1S=.1
0088 RRM=13.08*PHC *PI1A/V1S
0089 1C1K=1C-1K
0090 1MB1K=1MB-1K
0091 IF(1C1K,11,1) 1C1K=.2) 1C1K=.2
0092 IF(1MB1K,11,1) 1MB1K=.1
0093 AL=ALOG(1C1K)/(1MB1K)
0094 1C1AR=1U+(1C-1A)/A1
0095 151K1=15-1K1
0096 IF(151K1,11,1) 151K1=.1
0097 GPO=525.-11.*R*1V1S+.0969*1V1S**2
0098 IF(GPO,11,1) GPO=1.
0099
0100

```

```

C   RA AND GR DO NOT INCLUDE T45R
0101   RA=GR0*VIS/.70
0102   H4=399.*.127*2.445/1.42*(RA+145F)**.29
0103   IF(H4 .LT. 77R.) H4=77R.
0104   GR(1)=GR0*.52
0105   GR(2)=GR0*1.7
0106   GR(3)=GR(2)
0107   TAB(1)=TA
0108   TAB(2)=TB
0109   TAB(3)=TB
0110   U(1)=UA
0111   U(2)=UP
0112   U(3)=UB
0113   T(1)=T1
0114   T(2)=T2
0115   T(3)=T3
0116   DO 66 I=1,3
0117   DELT=.5*(T(I)-TAB(I)+TX(I)-TWR)
0118   IF(DELT .LT. .1) DELT=.1
0119   REP=RHO*U(I)*X(I)/VIS*.0275*(GR(I)+DELT)**.8/(X(I)*VIS)**.2
0120   IF(REP .LT. 1.) REP=1.
0121   NU(I)=2.246*.7R4*(REP*VIS*X(I))**.333
0122   66   H(I)=31.7*R(I)*NU(I)/X(I)
0123   H1=H(1)
0124   H2=H(2)
0125   H3=H(3)
0126   DO 15 I=1,21
0127   15   R(I)=0.
0128   B(2)=-RDM*ICPAR
0129   B(3)=-RDM*ICPAR
0130   B(4)= CI
0131   B(5)= CO
0132   B(6)=UA*(TA-TWR)
0133   B(7)=UP*(TB-TWR)
0134   B(8)=UC*(TC-TWR)
0135   TFI=(TWT+15)/2.
0136   ZI=.25*TFI+15.7
0137   B(11)=TWT*10P*ZI*(T5TWT)**.333+CI+CO
0138   B(16)=CO
0139   B(17)=CI
0140   B(21)=IM*2.
0141   A(2,6)=-RDM/2.
0142   A(2,18)=-RDM/2.
0143   A(3,7)=-RDM/2.
0144   A(3,18)=-RDM/2.
0145   A(6,6)=UA
0146   A(6,18)=-UA
0147   A(6,20)=TA-TWR
0148   A(7,7)=UP
0149   A(7,18)=-UP
0150   A(7,20)=TB-TWR
0151   A(8,8)=UC
0152   A(8,18)=-UC
0153   A(8,21)=TC-TWR
0154   A(11,13)=10P*ZI+15TWT**.333
0155   A(12,4)=-2./H4

```

```

0156 A(I,3)=-2./F3
0157 A(I,2)=-2./F2
0158 A(I,1)=-2./H1
0159 A(I,7)=-H3
0160 A(I,8)=-H4
0161 A(I,11)=H3
0162 A(I,12)=H4
0163 A(I,6)=-H1
0164 A(I,7)=-H2
0165 A(I,9)=H1
0166 A(I,10)=H2
0167 A(I,7)=-.00263*H3
0168 A(I,8)=-.00222*H4
0169 A(I,11)=-1.-.00263*H3
0170 A(I,12)=1.-.00222*H4
0171 A(I,6)=-.00451*H1
0172 A(I,7)=-.00308*H2
0173 A(I,9)=-1.-.00645*H1
0174 A(I,10)=1.-.00308*H2
0175 DO 50 I=1,21
0176 DO 50 J=1,21
0177 AA(I,J)=A(I,J)
0178 CALL MINVS(AA,N,AM,C,B,K)
0179 WRITE(6,10)P(1),I=3,21
0180 FORMAT(IX,3F7.0,16E6.1)
0181 WRITE(6,9) P(1),B(2),D,ICPAR,RA,(NU(I),I=1,3),(H(I),I=1,3),H4,TH
0182 FORMAT( ' Q=',2F7.0, ' D=',E11.4, ' ICPAR=',F6.1, ' RA=',E11.4,
* ' NU=',3F6.2, ' H=',4E6.0, ' TW=',F6.1)
0183 IF(KK .LT. 6) GC IC 90
0184 K2=EL0AT(KK)/2.-KK/2
0185 IF(K2 .GT. .1) GC IC 90
0186 DO 92 I=1,21
0187 R(I)=(R(I)+C(I))/2.
0188 CONTINUE
0189 DO 91 I=1,21
0190 C(I)=R(I)
0191 VA=B(I)
0192 UB=R(2C)
0193 HXX=ABS(LUR-UPP)
0194 IF(UXX .LT. .1) JJ=1
0195 UNO=UB
0196 UC=B(2I)
0197 T45B=(R(I)-P(I)+B(I))-R(I)/2.
0198 IF(T45B .LT. .1) T45B=.1
0199 T5=B(I)
0200 TMB=B(I)
0201 TA=B(6)
0202 TB=B(7)
0203 TC=B(8)
0204 TL=B(9)
0205 T2=B(10)
0206 T3=B(11)
0207 T4=B(12)
0208 O5=B(5)
0209 DO 55 I=1,3
0210 TX(I)=R(I)

```

```
0211      IF(C5 .LT. 1.) C5=1.
0212      DO 96 I=1,4
0213      Z=.25*W+15.7
0214      TM=(W+1.0711*(C5/Z))**.75
0215      96  TF=(TM+W)/2.
0216      65  CONTINUE
0217      IF(KK .LT. 20) GO TO 60
0218      DO 41 I=6,18
0219      B(I)=(P(I)-32.1)/1.E
0220      61  DT(I)=P(I)-TWC
0221      WRITE(6,91)
0222      WRITE(6,101)(P(I),I=3,21)
0223      WRITE(6,70)(XP(I),I=1,9)
0224      70  FORMAT(' EXPERIMENTAL DATA',4X,4F6.1,6X,
*F6.1,36X,4F6.1,/)
0225      WRITE(6,72)(DT(I),I=6,21)
0226      72  FORMAT(' CALC. TEMP. DIFF.',4X,16F6.1)
0227      DO 62 I=1,6
0228      62  XP(I)=XP(I)-TWC
0229      WRITE(6,70)(XP(I),I=1,9)
0230      60  CONTINUE
0231      GO TO 14
0232      13  STOP
0233      END
```

52



099. 5238. 7149. 142.4 139.5 141.2 143.0 142.5 138.7 137.1 125.3 121.0 121.1 122.4 122.3 119.0 154.4 221.9 198.0  
 O= 635. 1661. D= 0.29320+06 TCBAR= 124.0 RA= 0.1573E+04 NU= 3.07 3.47 3.44 H= 479. 651. 753. 1146. TM= 119.2  
 1095. 5233. 7149. 142.4 139.5 141.2 143.0 142.5 138.7 137.1 125.3 121.0 121.1 122.4 122.2 119.0 154.5 222.5 198.5  
 Q= 634. 1661. D= 0.29660+06 TCBAR= 124.0 RA= 0.1972E+04 NU= 3.07 3.48 3.45 H= 479. 652. 755. 1146. TM= 119.2  
 1006. 5232. 7149. 142.3 139.4 141.2 143.0 142.5 138.7 137.1 125.3 121.0 121.1 122.4 122.2 119.0 154.5 222.6 198.6  
 Q= 634. 1661. D= 0.29690+06 TCBAR= 124.0 RA= 0.1971E+04 NU= 3.07 3.48 3.45 H= 479. 652. 755. 1146. TM= 119.2

Q3	Q4	Q5	IA	IB	IC	II	I2	I3	I4	I5	I1B	I2B	I3B	I4B	I5B	UA	UB	UC
1005.	5232.	7149.	61.3	59.7	55.1	61.7	61.4	59.3	58.4	51.8	49.5	49.5	50.2	50.1	40.3	154.5	222.5	198.5
EXPERIMENTAL DATA			58.4	57.6	0.0	58.1		57.2								49.0	0.0	0.0
CALC. TEMP. DIFF.			16.3	14.7	10.1	16.7	16.4	14.3	13.4	6.8	4.5	4.5	5.2	5.1	3.3	0.0	0.0	0.0
EXPERIMENTAL DATA			13.4	12.6	-45.0	13.1		12.2								4.0	0.0	0.0

POWER	QU	Q1	TWC	TWC	TW	TWT	TF	TM	TCP
3.3	8233.1	3029.7	45.2	45.2	113.4	113.4	117.7	122.0	1.076

Q3	Q4	Q5	IA	IB	IC	II	I2	I3	I4	I5	I1B	I2B	I3B	I4B	I5B	UA	UB	UC
0.	0.	10137.	141.1	141.1	135.9	142.1	142.1	142.1	142.1	130.7	121.0	121.0	121.0	0.0	118.4	94.6	189.2	189.2
1781.	6452.	9479.	145.5	141.8	132.9	146.5	145.9	142.7	140.5	127.3	126.1	126.2	127.8	127.6	123.4	217.9	332.3	293.6
Q=	860.	2169.	D= 0.28790+06	TCBAR= 125.0	RA= 0.2009E+04	NU= 2.97	3.41	3.41	H= 464.	639.	746.	1196.	TM= 122.0					
1437.	6796.	9492.	148.7	145.3	135.5	149.6	149.1	144.7	142.7	128.4	123.2	123.2	124.9	124.7	120.7	165.5	220.1	199.3
Q=	872.	2158.	D= 0.49740+06	TCBAR= 128.0	RA= 0.2078E+04	NU= 3.17	3.65	3.63	H= 495.	684.	754.	1221.	TM= 121.0					
1482.	6751.	9441.	147.9	144.5	135.2	148.9	148.4	144.1	142.1	128.3	123.2	123.2	124.9	124.6	120.6	183.4	257.3	230.6
Q=	885.	2145.	D= 0.39710+06	TCBAR= 126.8	RA= 0.2075E+04	NU= 3.09	3.49	3.46	H= 483.	655.	757.	1232.	TM= 121.0					
1525.	6709.	9445.	147.8	144.4	135.2	148.8	148.2	144.1	142.2	128.3	123.1	123.2	124.8	124.5	120.5	183.9	261.8	234.0
Q=	883.	2147.	D= 0.44140+06	TCBAR= 126.6	RA= 0.2065E+04	NU= 3.12	3.55	3.52	H= 487.	645.	770.	1224.	TM= 121.0					
1531.	6702.	9445.	147.7	144.4	135.2	148.8	148.2	144.1	142.1	128.3	123.1	123.2	124.8	124.5	120.5	184.0	262.7	234.7
Q=	882.	2147.	D= 0.44570+06	TCBAR= 126.5	RA= 0.2064E+04	NU= 3.12	3.56	3.53	H= 488.	666.	772.	1224.	TM= 121.0					
1532.	6701.	9445.	147.7	144.4	135.2	148.8	148.2	144.1	142.1	128.3	123.1	123.2	124.8	124.5	120.5	184.0	262.7	234.7
Q=	882.	2147.	D= 0.44610+06	TCBAR= 126.5	RA= 0.2063E+04	NU= 3.12	3.56	3.53	H= 488.	666.	772.	1224.	TM= 121.0					

Q3	Q4	Q5	IA	IB	IC	II	I2	I3	I4	I5	I1B	I2B	I3B	I4B	I5B	UA	UB	UC	
1532.	6702.	9445.	64.3	62.4	57.4	64.9	64.6	62.3	61.2	53.5	50.6	50.6	51.5	51.4	49.2	184.0	262.7	234.7	
EXPERIMENTAL DATA			62.1	60.7	58.3	0.0		0.0								48.7	0.0	236.0	0.0
CALC. TEMP. DIFF.			19.1	17.2	12.2	19.7	19.4	17.1	16.0	8.3	5.4	5.4	6.3	6.2	4.0	0.0	0.0	0.0	
EXPERIMENTAL DATA			16.9	15.5	13.1	-45.2		-45.2								3.5	0.0	236.0	0.0

POWER	QU	Q1	TWC	TWC	TW	TWT	TF	TM	TCP
3.6	8981.6	3305.1	48.0	48.0	118.4	118.4	122.9	127.4	1.076

Q3	Q4	Q5	IA	IB	IC	II	I2	I3	I4	I5	I1B	I2B	I3B	I4B	I5B	UA	UB	UC
0.	0.	11058.	147.6	147.6	142.0	148.6	148.6	148.6	148.6	136.5	126.2	126.2	126.2	0.0	123.4	98.2	196.4	196.4
2049.	6932.	10362.	150.8	147.1	135.5	152.0	151.4	147.9	146.2	132.7	131.8	131.8	133.5	133.2	128.8	236.2	357.4	316.2
Q=	967.	2338.	D= 0.35570+06	TCBAR= 130.4	RA= 0.2185E+04	NU= 2.98	3.43	3.43	H= 466.	643.	750.	1249.	TM= 127.4					
1696.	7286.	10350.	154.5	151.2	141.5	155.7	155.1	150.9	148.8	134.1	128.7	128.7	130.4	130.2	125.9	180.8	239.0	216.5
Q=	977.	2329.	D= 0.57870+06	TCBAR= 133.5	RA= 0.2246E+04	NU= 3.19	3.69	3.67	H= 499.	651.	603.	1259.	TM= 126.4					
1729.	7262.	10306.	153.8	150.3	141.1	155.0	154.4	150.2	148.2	134.0	128.7	128.8	130.5	130.2	125.9	200.8	280.3	251.5
Q=	989.	2316.	D= 0.48980+06	TCBAR= 122.3	RA= 0.2247E+04	NU= 3.12	3.53	3.50	H= 487.	662.	766.	1275.	TM= 126.4					
1763.	7219.	10311.	153.7	150.2	141.1	154.9	154.3	150.2	148.2	134.0	128.6	128.7	130.4	130.1	125.8	201.0	284.7	254.7
Q=	986.	2319.	D= 0.54700+06	TCBAR= 122.1	RA= 0.2237E+04	NU= 3.15	3.59	3.57	H= 492.	673.	779.	1267.	TM= 126.3					
1770.	7211.	10311.	153.6	150.2	141.1	154.9	154.2	150.2	148.2	134.0	128.6	128.7	130.4	130.1	125.8	201.3	285.7	255.6
Q=	986.	2319.	D= 0.55210+06	TCBAR= 122.0	RA= 0.2236E+04	NU= 3.15	3.59	3.57	H= 492.	674.	781.	1267.	TM= 126.3					
1771.	7210.	10311.	153.6	150.2	141.1	154.8	154.2	150.2	148.2	134.0	128.6	128.7	130.4	130.1	125.8	201.2	285.8	255.6
Q=	986.	2319.	D= 0.55270+06	TCBAR= 132.0	RA= 0.2235E+04	NU= 3.15	3.60	3.57	H= 492.	674.	781.	1267.	TM= 126.3					

Q3	Q4	Q5	IA	IB	IC	II	I2	I3	I4	I5	I1B	I2B	I3B	I4B	I5B	UA	UB	UC	
1771.	7211.	10311.	67.6	65.7	60.6	68.2	67.9	65.7	64.5	56.7	53.7	53.7	54.6	54.5	52.1	201.2	285.8	255.6	
EXPERIMENTAL DATA			66.6	65.9	55.0	74.0		65.5								53.0	0.0	0.0	0.0
CALC. TEMP. DIFF.			19.6	17.7	12.6	20.2	19.9	17.7	16.5	8.7	5.7	5.7	6.6	6.5	4.1	0.0	0.0	0.0	

54

```

C
C PROGRAM SHAPE
0001 DIMENSION T(20),TS(20),PS(20),APS(20)
0002 READ(5,4)(PS(I),I=1,10)
0003 READ(5,4)(PS(I),I=11,20)
0004 4 FORMAT(10F6.3)
0005 WRITE(6,5)
0006 5 FORMAT(/,,' POWER PROFILE')
0007 WRITE(6,4)(PS(I),I=1,10)
0008 WRITE(6,4)(PS(I),I=11,20)
0009 23 READ(5,1) A,P,TWC,F,TL,TWB,TP,TMB,C
0010 1 FORMAT(A4,7F4.1,F8.0)
0011 IF(P.EQ.0.) GO TO 21
0012 WRITE(6,2)
0013 2 FORMAT(/,,' TYPE',,' P',3X,'TWC',3X,'H',4X,'TL',4X,'TWB',3X,'TM',
*,4X,'TMB',5X,'C')
0014 WRITE(6,1) A,P,TWC,F,TL,TWB,TP,TMB,Q
0015 TILT=(TM-TL)*2./(TP-TL+TMB-TWB)
0016 SP=0.
0017 TMAX=0.
0018 DO 7 I=1,20
0019 APS(I)=PS(I)*(1.+(TILT-1.)*(10.5-FLCAT(I)))/5.5)
0020 7 SP=SP+APS(I)
0021 DO 20 I=1,20
0022 20 APS(I)=APS(I)*20./SP
0023 T(I)=TL
0024 DO 8 I=2,20
0025 8 T(I)=1(I-1)-(APS(I)+APS(I-1))/2.*(TL-TWB)/19.
0026 DO 9 I=1,20
0027 TS(I)=T(I)+APS(I)*C/H
0028 IF(TS(I).GT.TMAX) TMAX=TS(I)
0029 9 CONTINUE
0030 TMAX=(TMAX-32.)/1.8
0031 WRITE(6,10) TILT,SP
0032 10 FORMAT(' TILT=',F7.2,' SP=',F7.3,4X,'APS')
0033 WRITE(6,4)(APS(I),I=1,10)
0034 WRITE(6,4)(APS(I),I=11,20)
0035 WRITE(6,15)
0036 15 FORMAT(/,,' T')
0037 WRITE(6,13)(T(I),I=1,20)
0038 13 FORMAT(20F6.1)
0039 WRITE(6,14) TMAX
0040 14 FORMAT(' TS',5X,'TMAX=',F6.1)
0041 WRITE(6,13)(TS(I),I=1,20)
0042 GO TO 23
0043 21 CONTINUE
0044 END

```

## POWER PROFILE

0.351 0.460 0.782 0.959 1.100 1.205 1.265 1.290 1.300 1.300  
 1.300 1.300 1.290 1.265 1.215 1.152 1.075 0.957 0.807 0.630

TYPE P TWC H TL TWB TM TMB C  
 31A 20.0 30.0 530.0 191.6 107.4 202.8 122.5 6940.  
 TILT= 0.852 SP= 21.128 APS  
 0.283 0.378 0.654 0.816 0.952 1.061 1.132 1.173 1.202 1.221  
 1.240 1.259 1.269 1.263 1.231 1.184 1.121 1.012 0.865 0.685

T  
 191.6 190.1 187.9 184.6 180.7 176.2 171.4 166.3 161.0 155.6 150.2 144.6 139.0 133.4 127.9 122.5 117.4 112.7 108.5 105.1  
 TS TMAX= 91.3  
 195.3 195.1 196.4 195.3 193.1 190.1 186.2 181.6 176.7 171.6 166.4 161.1 155.6 150.0 144.0 138.0 132.1 126.0 119.9 114.1

TYPE P TWC H TL TWB TM TMB C  
 31A 20.0 40.0 536.0 200.9 124.8 212.3 139.6 7030.  
 TILT= 0.870 SP= 21.112 APS  
 0.289 0.385 0.665 0.828 0.964 1.071 1.141 1.180 1.206 1.223  
 1.240 1.257 1.264 1.256 1.222 1.173 1.109 0.999 0.852 0.674

T  
 200.9 199.5 197.4 194.5 190.9 186.8 182.4 177.7 172.9 168.1 163.1 158.1 153.1 148.0 143.1 138.3 133.7 129.5 125.8 122.7  
 TS TMAX= 96.8  
 204.7 204.6 206.2 205.3 203.5 200.8 197.3 193.2 188.8 184.1 179.4 174.6 169.7 164.5 159.1 153.7 148.3 142.6 137.0 131.6

TYPE P TWC H TL TWB TM TMB C  
 31A 16.0 50.0 532.0 201.2 137.8 210.2 154.4 5598.  
 TILT= 0.703 SP= 21.253 APS  
 0.232 0.318 0.563 0.719 0.857 0.975 1.060 1.119 1.166 1.204  
 1.242 1.281 1.309 1.321 1.304 1.270 1.217 1.112 0.961 0.769

T  
 201.2 200.3 198.8 196.7 194.0 191.0 187.6 184.0 180.1 176.2 172.1 167.9 163.6 159.2 154.8 150.5 146.4 142.5 139.0 136.1  
 TS TMAX= 96.0  
 203.6 203.6 204.7 204.2 203.1 201.2 198.7 195.7 192.4 188.9 185.2 181.4 177.3 173.1 168.5 163.9 159.2 154.2 149.1 144.2

TYPE P TWC H TL TWB TM TMB C  
 31B 16.0 30.0 842.0 169.2 113.4 184.7 134.8 15551.  
 TILT= 0.840 SP= 21.138 APS  
 0.279 0.373 0.647 0.808 0.944 1.054 1.126 1.169 1.195 1.220  
 1.240 1.261 1.272 1.267 1.237 1.191 1.128 1.020 0.872 0.691

T  
 169.2 168.2 166.7 164.6 162.0 159.1 155.9 152.5 149.1 145.5 141.9 138.2 134.5 130.8 127.1 123.5 120.1 117.0 114.2 111.9  
 TS TMAX= 82.0  
 174.4 175.1 178.7 179.5 179.5 178.6 176.7 174.1 171.2 168.0 164.8 161.5 158.0 154.2 149.9 145.5 141.0 135.8 130.3 124.7

TYPE P TWC H TL TWB TM TMB C  
 31B 16.0 40.0 856.0 180.4 129.9 196.1 150.9 15703.  
 TILT= 0.856 SP= 21.125 APS  
 0.284 0.379 0.656 0.818 0.954 1.063 1.134 1.175 1.202 1.221  
 1.240 1.259 1.268 1.261 1.229 1.182 1.118 1.009 0.863 0.683

T  
 180.4 179.5 178.1 176.2 173.8 171.1 168.2 165.2 162.0 158.8 155.5 152.2 148.8 145.5 142.2 139.0 135.9 133.1 130.6 128.5  
 TS TMAX= 88.5  
 185.6 186.5 190.2 191.2 191.3 190.6 189.0 186.7 184.1 181.2 178.2 175.3 172.1 168.6 164.7 160.6 156.4 151.6 146.4 141.0

56

TYPE TWC F TL TWB TM TMB C  
318 16.0 50.0 871.0 192.5 146.9 206.5 167.4 15879.  
TILT= 0.877 SP= 21.107 APS  
0.292 0.388 0.669 0.832 0.968 1.075 1.144 1.183 1.206 1.224  
1.240 1.256 1.267 1.253 1.219 1.170 1.105 0.995 0.849 0.671

T  
192.5 191.7 190.4 188.6 186.5 184.0 181.3 178.5 175.7 172.8 169.8 166.8 163.8 160.8 157.8 154.9 152.2 149.7 147.5 145.7  
TS TMAX= 95.6  
157.8 198.8 202.6 203.8 204.1 203.6 202.2 200.1 197.7 195.1 192.4 189.7 186.8 183.6 180.0 176.3 172.3 167.8 163.0 157.5

TYPE P TWC H TL TWB TM TMB C  
16 20.0 30.0 706.0 181.2 104.4 200.2 123.5 13466.  
TILT= 0.997 SP= 21.005 APS  
0.333 0.437 0.743 0.911 1.046 1.146 1.203 1.227 1.237 1.238  
1.238 1.238 1.229 1.206 1.158 1.059 1.025 0.913 0.770 0.601

T  
181.2 179.6 177.3 173.9 170.0 165.5 160.8 155.9 150.9 145.9 140.9 135.9 130.9 126.0 121.2 116.6 112.3 108.4 105.0 102.2  
TS TMAX= 88.6  
187.6 188.0 151.4 191.3 189.9 187.4 183.7 179.3 174.5 169.5 164.5 159.5 154.3 149.0 143.3 137.6 131.5 125.8 119.7 113.7

TYPE P TWC H TL TWB TM TMB C  
16 20.0 40.0 716.0 191.7 122.3 210.5 141.1 13471.  
TILT= 1.000 SP= 21.003 APS  
0.334 0.438 0.745 0.913 1.047 1.147 1.205 1.228 1.238 1.238  
1.238 1.238 1.228 1.205 1.157 1.097 1.024 0.911 0.768 0.600

T  
191.7 190.3 188.1 185.1 181.5 177.5 173.2 168.8 164.3 159.7 155.2 150.7 146.2 141.8 137.4 133.3 129.5 125.9 122.9 120.4  
TS TMAX= 94.6  
198.0 198.5 202.1 202.3 201.2 199.1 195.9 191.9 187.6 183.0 178.5 174.0 169.3 164.4 159.2 154.0 148.7 142.1 137.3 131.6

TYPE P TWC H TL TWB TM TMB C  
16 20.0 50.0 724.0 203.3 140.3 221.9 158.9 13474.  
TILT= 1.000 SP= 21.003 APS  
0.334 0.438 0.745 0.913 1.047 1.147 1.205 1.228 1.238 1.238  
1.238 1.238 1.228 1.205 1.157 1.097 1.024 0.911 0.768 0.600

T  
203.3 202.0 200.1 197.3 194.1 190.4 186.5 182.5 178.4 174.3 170.2 166.1 162.0 158.0 154.0 150.3 146.8 143.6 140.8 138.5  
TS TMAX= 101.3  
209.5 210.2 213.9 214.3 213.6 211.8 208.9 205.3 201.4 197.3 193.2 189.1 184.9 180.4 175.6 170.7 165.8 160.5 155.1 145.7

TYPE P TWC H TL TWB TM TMB C  
53 20.0 30.0 1231.0 177.6 120.7 185.6 137.5 15250.  
TILT= 0.645 SP= 21.302 APS  
0.213 0.295 0.529 0.682 0.821 0.941 1.032 1.098 1.152 1.198  
1.243 1.289 1.324 1.343 1.332 1.304 1.254 1.150 0.998 0.801

T  
177.6 176.8 175.6 173.8 171.5 168.9 166.0 162.8 159.4 155.9 152.2 148.4 144.5 140.5 136.5 132.6 128.7 125.1 121.9 119.2  
TS TMAX= 83.5  
180.2 180.5 182.2 182.2 181.7 180.6 178.7 176.4 173.7 170.7 167.6 164.4 160.9 157.2 153.0 148.7 144.3 139.4 134.3 129.2

TYPE P TWC H TL TWB TM TMB C  
53 20.0 40.0 1247.0 188.5 136.6 197.0 153.0 15530.  
TILT= 0.683 SP= 21.270 APS  
0.225 0.310 0.551 0.706 0.844 0.963 1.050 1.112 1.161 1.202  
1.243 1.284 1.314 1.329 1.314 1.282 1.230 1.125 0.974 0.780

T  
188.5 187.8 186.6 184.9 182.8 180.3 177.5 174.6 171.5 168.3 164.9 161.5 157.9 154.3 150.7 147.2 143.7 140.5 137.6 135.2  
TS TMAX= 89.8  
191.3 191.6 193.5 193.7 193.3 192.3 190.6 188.4 185.5 183.2 180.4 177.5 174.3 170.9 167.1 163.1 159.0 154.5 149.8 145.0

TYPE P TWC H TL TWR TM TMB C  
53 20.0 50.01263.0 200.3 152.9 209.4 169.0 15840.  
TILT= 0.722 SP= 21.237 APS  
0.239 0.326 0.575 0.731 0.869 0.986 1.069 1.126 1.171 1.206  
1.242 1.278 1.304 1.313 1.295 1.259 1.205 1.099 0.949 0.758

T  
200.3 195.6 198.5 196.8 194.8 192.5 190.0 187.2 184.4 181.4 178.3 175.2 172.0 168.7 165.5 162.3 159.2 156.3 153.8 151.6  
TS TMAX= 96.7  
203.3 203.7 205.7 206.0 205.7 204.5 203.4 201.4 199.0 196.5 193.9 191.2 188.3 185.2 181.7 178.1 174.3 170.1 165.7 161.2

TYPE P TWC H TL TWR TM TMB C  
15 20.0 30.0 673.0 183.0 117.3 199.2 136.0 11743.  
TILT= 0.928 SP= 21.063 APS  
0.309 0.409 0.701 0.866 1.001 1.105 1.165 1.202 1.220 1.230  
1.239 1.248 1.248 1.233 1.193 1.139 1.071 0.960 0.815 0.641

T  
183.0 181.8 179.8 177.1 173.9 170.3 166.3 162.2 158.0 153.8 149.5 145.2 140.9 136.6 132.4 128.4 124.6 121.1 118.0 115.5  
TS TMAX= 89.0  
188.4 188.9 192.1 192.2 191.4 189.5 186.7 183.2 179.3 175.3 171.2 167.0 162.7 158.1 153.3 148.3 143.3 137.8 132.2 126.7

TYPE P TWC H TL TWR TM TMB C  
15 20.0 40.0 683.0 192.8 133.4 205.0 151.8 11820.  
TILT= 0.936 SP= 21.056 APS  
0.312 0.412 0.705 0.871 1.006 1.110 1.173 1.205 1.222 1.231  
1.239 1.247 1.246 1.230 1.189 1.134 1.065 0.955 0.810 0.636

T  
192.8 191.7 189.9 187.5 184.5 181.2 177.6 173.9 170.1 166.3 162.4 158.6 154.7 150.8 147.0 143.4 139.9 136.8 134.0 131.8  
TS TMAX= 94.7  
198.2 198.8 202.1 202.5 201.9 200.4 198.0 194.8 191.2 187.6 183.9 180.1 176.2 172.1 167.6 163.0 158.4 153.3 148.0 142.8

TYPE P TWC H TL TWR TM TMB C  
15 20.0 50.0 693.0 203.7 150.0 219.9 168.1 11892.  
TILT= 0.945 SP= 21.050 APS  
0.315 0.415 0.711 0.877 1.012 1.115 1.177 1.208 1.224 1.232  
1.239 1.246 1.244 1.226 1.185 1.130 1.060 0.949 0.805 0.632

T  
203.7 202.7 201.1 198.8 196.2 193.2 189.5 186.6 183.1 179.6 176.2 172.6 169.1 165.6 162.2 159.0 155.9 153.0 150.5 148.5  
TS TMAX= 101.0  
209.1 205.8 213.3 213.9 213.5 212.3 210.1 207.3 204.1 200.8 197.4 194.0 190.5 186.7 182.6 178.3 174.1 169.3 164.4 159.4

```

C
C PROGRAM SHP31B
0001 DIMENSION T(20),TS(20),PS(20),APS(20),TCC(20),E(20),Q44(20)
0002 REAL K5(21)
0003 AC=.01253
0004 R4=.1542
0005 R5=.1671
0006 PI=3.14159
0007 RHO=67.0
0008 READ(5,4)(PS(I),I=1,10)
0009 READ(5,4)(PS(I),I=11,20)
0010 4 FORMAT(10F6.3)
0011 WRITE(6,5)
0012 5 FORMAT(/,' POWER PROFILE')
0013 WRITE(6,4)(PS(I),I=1,10)
0014 WRITE(6,4)(PS(I),I=11,20)
0015 23 READ(5,1) A,P,TWC,H,TB,TC,TWB,T3,T3B,Q3,Q4,UC
0016 1 FORMAT(A4,8F6.1,3F7.0)
0017 IF(P .EQ. 0.1 GC TO 21
0018 WRITE(6,2)
0019 2 FORMAT(/,' TYPE', ' P',3X,'TWC',3X,'H',5X,'TB',4X,'TC',4X,'TWB',
*3X,'T3',4X,'T3B',3X,'Q3',4X,'Q4',7X,'UC')
0020 WRITE(6,1) A,P,TWC,H,TB,TC,TWB,T3,T3B,Q3,Q4,UC
0021 TILT=(T3-TB)*2./(T3-TB+T3B-T3B)
0022 K=0
0023 SP=0.
0024 TMAX=0.
0025 TW=TWC*1.8+32.
0026 DO 7 I=1,20
0027 APS(I)=PS(I)*(1.+(TILT-1.)*(10.5-FLOAT(I))/9.5)
0028 7 SP=SP+APS(I)
0029 DO 20 I=1,20
0030 20 APS(I)=APS(I)*20./SP
0031 T(I)=TB
0032 DO 8 I=2,20
0033 8 T(I)=T(I-1)-(APS(I)+APS(I-1))/2.*(TB-TWB)/19.
0034 DO 9 I=1,20
0035 TS(I)=T(I)+APS(I)*Q3/H
0036 IF(TS(I) .GT. TMAX) TMAX=TS(I)
0037 9 CONTINUE
0038 TMAX=(TMAX-32.)/1.0
0039 WRITE(6,10) TILT,SP
0040 10 FORMAT(' TILT=',F7.3,' SP=',F7.3,4X,' APS')
0041 WRITE(6,4)(APS(I),I=1,10)
0042 WRITE(6,4)(APS(I),I=11,20)
0043 WRITE(6,15)
0044 15 FORMAT(/,' T')
0045 WRITE(6,13)(T(I),I=1,20)
0046 13 FORMAT(20F6.1)
0047 WRITE(6,14) TMAX
0048 14 FORMAT(' IS',5X,'TMAX=',F6.1)
0049 WRITE(6,13)(TS(I),I=1,20)
0050 K5(I)=(Q3+Q4)*.5+2./(TC+TWB-2.*TW)/(2.*PI*13.*R5)
0051 UAR=2.*PI*13.*.C5/UC/AC/RHC
0052 50 K=K+1
0053 TCC(I)=TC

```

```
0054      DO 51 I=2,20
0055      Q44(I)=(Q4+C3)*(PS(I)+PS(I-1))/2./13.-Q3*(APS(I)+APS(I-1))/2./13.
          */2./P1/R4
0056      51 TCC(I)=TCC(I-1)-(K5(K)*(TCC(I-1)-TW)*R5-Q44(I)*R4)*UAR
0057      E(K)=TCC(20)-TWB
0058      WRITE(6,60) K5(K)
0059      WRITE(6,13)(TCC(I),I=1,20)
0060      60 FORMAT(' K5=',E10.3,' TCC')
0061      IF(K .GT. 1) GO TO 52
0062      K5(2)=K5(1)*1.01
0063      GO TO 50
0064      52 K5(K+1)=K5(K)-E(K)/(E(K)-E(K-1))*(K5(K)-K5(K-1))
0065      DK5=ABS(K5(K+1)-K5(K))/K5(K)
0066      IF(K .EQ. 20) GO TO 23
0067      IF(DK5 .GT. .001) GO TO 50
0068      GO TO 23
0069      21 CONTINUE
0070      END
```

09

POWER PROFILE

0.351 0.460 0.782 0.959 1.100 1.205 1.265 1.290 1.300 1.300  
 1.300 1.300 1.290 1.265 1.215 1.152 1.075 0.957 0.807 0.630

TYPE P TWC H TB TC TWB T3 T3B Q3 Q4 UC  
 318 16.0 30.0 842.0 169.2 158.5 113.4 184.7 134.8 15551. 39057. 327.  
 TILT= 0.840 SP= 21.138 APS  
 0.279 0.373 0.647 0.808 0.944 1.054 1.126 1.169 1.195 1.220  
 1.240 1.261 1.272 1.267 1.237 1.191 1.126 1.020 0.873 0.691

T  
 169.2 168.2 166.7 164.6 162.0 159.1 155.9 152.5 149.1 145.5 141.9 138.2 134.5 130.8 127.1 123.5 120.1 117.0 114.2 111.9  
 TS TMAX= 82.0  
 174.4 175.1 178.7 179.5 179.5 178.6 176.7 174.1 171.2 168.0 164.8 161.5 158.0 154.2 149.9 145.5 141.0 135.8 130.2 124.7  
 K5= 0.721E+02 TCC  
 158.5 148.7 142.3 138.9 137.2 136.6 136.7 137.1 137.5 137.7 137.9 138.0 138.0 137.8 137.3 136.4 135.2 133.5 131.1 128.0  
 K5= 0.728E+02 TCC  
 158.5 148.6 142.1 138.6 136.8 136.2 136.4 136.7 137.0 137.3 137.5 137.5 137.5 137.3 136.8 135.9 134.7 133.0 130.6 127.5  
 K5= 0.940E+02 TCC  
 158.5 144.8 135.9 130.9 128.2 127.0 126.6 126.6 126.6 126.6 126.6 126.5 126.3 126.0 125.5 124.6 123.4 121.7 119.5 116.6  
 K5= 0.100E+03 TCC  
 158.5 143.7 134.2 128.8 125.9 124.6 124.2 124.1 124.1 124.1 124.1 124.0 123.8 123.5 122.9 122.1 120.9 119.3 117.1 114.3  
 K5= 0.103E+03 TCC  
 158.5 143.3 133.5 128.0 125.1 123.8 123.3 123.2 123.2 123.2 123.2 123.1 122.9 122.6 122.0 121.2 120.0 118.4 116.2 113.5  
 K5= 0.103E+03 TCC  
 158.5 143.2 133.4 128.0 125.0 123.7 123.2 123.2 123.2 123.2 123.1 123.0 122.8 122.5 122.0 121.1 119.9 118.3 116.2 113.4

TYPE P TWC H TB TC TWB T3 T3B Q3 Q4 UC  
 318 16.0 40.0 856.0 180.4 170.9 129.9 196.1 150.9 15703. 38905. 366.  
 TILT= 0.856 SP= 21.125 APS  
 0.284 0.379 0.656 0.818 0.954 1.063 1.134 1.175 1.203 1.221  
 1.240 1.259 1.268 1.261 1.229 1.182 1.118 1.009 0.863 0.683

T  
 180.4 179.5 178.1 176.2 173.8 171.1 168.2 165.2 162.0 158.8 155.5 152.2 148.8 145.5 142.2 139.0 135.9 133.1 130.6 128.5  
 TS TMAX= 88.5  
 185.6 186.5 190.2 191.2 191.3 190.6 189.0 186.7 184.1 181.2 178.2 175.3 172.1 168.6 164.7 160.6 156.4 151.6 146.4 141.0  
 K5= 0.776E+02 TCC  
 170.9 162.2 156.5 153.3 151.7 151.2 151.2 151.5 151.7 152.0 152.1 152.2 152.1 152.0 151.5 150.8 149.7 148.2 146.0 143.2  
 K5= 0.784E+02 TCC  
 170.9 162.1 156.3 153.1 151.4 150.8 150.6 151.1 151.4 151.6 151.7 151.7 151.7 151.5 151.1 150.3 149.2 147.7 145.6 142.8  
 K5= 0.101E+03 TCC  
 170.9 158.8 150.8 146.2 143.7 142.5 142.0 141.9 141.5 141.9 141.8 141.7 141.5 141.2 140.7 140.0 138.9 137.4 135.4 132.8  
 K5= 0.107E+03 TCC  
 170.9 157.9 149.3 144.4 141.7 140.4 139.9 139.7 139.7 139.6 139.5 139.4 139.3 139.0 138.5 137.7 136.6 135.2 133.2 130.7  
 K5= 0.110E+03 TCC  
 170.9 157.5 148.8 143.8 141.0 139.6 139.1 139.0 138.9 138.8 138.8 138.6 138.5 138.2 137.7 136.9 135.9 134.4 132.5 130.0  
 K5= 0.110E+03 TCC  
 170.9 157.5 148.7 143.7 140.9 139.6 139.0 138.9 138.8 138.8 138.7 138.6 138.4 138.1 137.6 136.9 135.8 134.4 132.4 129.9

TYPE P TWC H TB TC TWB T3 T3B Q3 Q4 UC  
 318 16.0 50.0 871.0 192.5 184.2 146.9 208.5 167.4 15879. 38729. 408.  
 TILT= 0.877 SP= 21.107 APS  
 0.292 0.388 0.669 0.832 0.968 1.075 1.144 1.183 1.208 1.224  
 1.240 1.256 1.262 1.253 1.219 1.170 1.105 0.995 0.845 0.671

T  
 192.5 191.7 190.4 188.6 186.5 184.0 181.3 178.5 175.7 172.8 169.8 166.8 163.8 160.8 157.8 154.9 152.2 149.7 147.5 145.7  
 TS TMAX= 95.6  
 197.8 198.8 202.6 203.8 204.1 203.6 202.2 200.1 197.7 195.1 192.4 189.7 186.8 183.6 180.0 176.3 172.3 167.8 163.0 157.9

19

K5= 0.827E+02 TCC  
184.2 176.5 171.3 168.4 166.9 166.3 166.3 166.5 166.7 166.9 167.0 167.1 167.0 166.9 166.5 165.9 164.9 163.5 161.6 159.1  
K5= 0.835E+02 TCC  
184.2 176.4 171.1 168.2 166.6 166.0 166.0 166.2 166.4 166.5 166.6 166.7 166.6 166.5 166.1 165.4 164.5 163.1 161.2 158.6  
K5= 0.107E+03 TCC  
184.2 173.5 166.4 162.2 159.8 158.6 158.0 157.9 157.8 157.7 157.6 157.5 157.3 157.1 156.6 155.9 155.0 153.6 151.8 149.5  
K5= 0.113E+03 TCC  
184.2 172.7 165.1 160.6 158.0 156.7 156.2 155.9 155.8 155.7 155.6 155.5 155.3 155.1 154.6 153.9 153.0 151.7 149.9 147.6  
K5= 0.116E+03 TCC  
184.2 172.4 164.6 160.1 157.4 156.1 155.5 155.3 155.2 155.1 155.0 154.8 154.7 154.4 154.0 153.3 152.3 151.0 149.2 147.0  
K5= 0.116E+03 TCC  
184.2 172.4 164.6 160.0 157.4 156.1 155.5 155.2 155.1 155.0 154.9 154.8 154.6 154.4 153.9 153.2 152.3 151.0 149.2 146.9

62